Coupled Systems Mechanics, *Vol. 14, No. 2 (2025) 129-159*
https://doi.org/10.12989/csm.2025.14.2.129

Modeling memory-dependent derivative on photothermoelastic half space in the presence of non-local and hyperbolic two temperatures

Rajneesh Kumar[1], Nidhi Sharma[2] and Supriya Chopra[*3]

[1]*Department of Mathematics, Kurukshetra University, Kurukshetra, Haryana, India*
[2]*Department of Mathematics, Maharishi Markandeshwar University Mullana, Ambala, Haryana, India*
[3]*Department of Mathematics, Government College for Women, Ambala City, Haryana, India*

(Received July 12, 2024, Revised April 6, 2025, Accepted April 9, 2025)

Abstract. The purpose of this paper is developed a new model of photothermoelastic with memory-dependent derivatives (PMDD) under non-local (NL) parameter, dual phase lag (DPL) and hyperbolic two temperature (HTT). The governing coupled equations of the considered model with time delay and kernel function, which can be chosen freely according to the necessity of applications, are applied to a two-dimensional problem of a half-space. Integral transform involving Laplace and Fourier transforms reduced the governing equations into ordinary differential equation. The arbitrary constants in the solution are determined by considering the loading environment on the surface. Three different categories of the sources are taken to explore the application as (i) normal force (ii) thermal source (iii) carrier density source. In the new domain, the closed form expressions of physical quantities like displacement, normal stress, conductive temperature field and carrier density distribution are derived. The numerical inversion method is employed to recover the results in a physical domain. The impact of non-local parameter, dual phase lag and hyperbolic two-temperature with and without MDD (memory dependent derivative) along with variations of all kernel functions on physical field variables are presented in form of graphs. Unique cases are also explored. The problem assumes great significance in an earthquake region when we think of variation of particle motion as a possible precursor for earthquake prediction. The results obtained are also helpful in designing the semiconductor materials in the course of coupled elastic, thermal, plasma waves and also find the application in the material and engineering sciences.

Keywords: dual phase lag; hyperbolic two temperature; kernel; memory-dependent derivative; non-local parameter; time delay

1. Introduction

Study of mechanical and thermal interaction within a solid medium is of emended significance in numerous fields of science. There are few examples such as high energy particle accelerated devices, modern aeronautical and astronomical engineering and different system utilized in nuclear and industrial utilization with the consideration of second sound effect in thermoelastic model

*Corresponding author, Assistant Professor, E-mail: chopra.s22@gmail.com

http://www.techno-press.org/?journal=csm&subpage=8 ISSN: 2234-2184 (Print), 2234-2192 (Online)

plays a vital role in analysing elastic body with in a variety of scientific and technological fields. The infinite thermal propagation speed is observed through conventional uncoupled theories in contradiction with physical observation. Biot (1956) proposed the coupled thermoelasticity in pursuance to remove the classic uncoupled principle’s inherent paradox. This paradox suggests no impact of temperature on elastic change. The heat equations for both diffusion theories indicate that the heat wave propagation rates are distinct physical considerations. Generalized thermoelasticity theories are intend to solve the delicacy and limitations essential in classic dynamic thermoelasticity coupled theory, which allow the thermal signal to propagate with unlimited speed.

The theory of generalized thermoelasticity considers the effect of the coupling between strain rate and temperature into account, but the evolving coupling equations are hyperbolic. Thus, the inconsistency in the classic combined theory bring out with regard to the infinite speed of heat propagation. One of the generalized theories of thermoelasticity updated, which included the implementation of a new thermal conductivity law to replace the Fourier conventional law was proposed by Lord and Shulman (1967). This amended legislation involves heat flow and its time-related partial derivative.

Green and Naghdi (1991, 1992, 1993) derived three models in thermoelasticity which are labelled as GN-I, II and III models. The linearized form of model-I reduces to classical heat conduction theory whereas linearized version of model-II and III permit propagation of thermal waves at finite speed.GN-II (1993) shows a feature which makes it different from other thermoelastic models as it does not allow dissipation of thermal energy. The model GN-III (1992) contains the thermal displacement gradient alongwith temperature gradient among the constitutive variables and admits the dissipation of energy.

Tzou (1995) developed the DPL model to describe the description of phase lag between temperature gradient and heat flux has been incorporated.

The semiconducting materials were used widely in advanced engineering, with the development of technologies. The study of wave propagation in a semiconducting medium will have important academic significance and application value. Of recent interest is the relevance of the excitation of short elastic pulses (high-frequency elastic waves) by photothermal means to several areas of applied physics including the photoacoustic microscope, thermal wave imaging, determination of thermoelastic material parameters, non-destructive evaluation of devices, monitoring of laser drilling, and laser annealing and melting phenomena in semiconductors. During the last few years, photoacoustic (PA) and photothermal (PT) science and technology have significantly evolved new methods in the investigation of semiconductors and microelectronic structures. PA and PT techniques were recently established as diagnostic methods with good delicacy to the dynamics of photoexcited carrier (Mandelis 1987, Almond and Patel 1996, Mandelis and Michaelian 1997, Nikolic and Todorovic 1989).

Several researchers (McDonald and Wetsel 1978, Jackson and Amer 1980, Steams and Kino 1985) analysed the difference of thermoelastic and electronic deformations in semiconductor media by set aside the coupling between the plasma and the thermoelastic equations. (Todorovic 2003a, 2003b, 2005) presented two phenomena to dispense information about the properties of transport and carrier recombinations in the semiconducting medium. The changes in the propagations of thermal and plasma waves revert to the linear coupling between the thermal and the mass transport (i.e., thermodiffusion) have included. Sharma (2010) investigated the boundary value problems in generalized thermodiffusive elastic medium. Sharma *et al.* (2013) studied the propagation of plane wave in anisotropic thermoviscoelastic medium in the context of the theory

GN type-II and GN type-III. Sharma and Sharma (2014) investigated the temperature inconstancy in tissues based on Penne's bio-heat transfer equation.

Lotfy *et al.* (2018) investigated the interaction between a magnetic field and elastic materials with microstructure, whose microelements possess microtemperatures with photothermal excitation. Jahangir *et al.* (2020) discussed the reflection of thermoelastic waves in semiconducting medium. Abouelregal *et al.* (2021) introduced a new mathematical model for functionally graded thermoelastic nanobeams (FGNB) which contains a free choice of the kernel function and time delay. Abouelregal *et al.* (2022) discussed the vibrational behavior of rotating nanobeams with variable thermal properties to analyzed through a memory-dependent derivative heat conduction model. Abouelregal *et al.* (2023) studied to explores the impact of the non-local Moore-Gibson-Thompson (MGT) heat transfer model on thermoelastic materials, incorporating memory-dependent derivatives. Abouelregal *et al.* (2024) investigated the transient thermoelastic response of a semi-infinite medium subjected to a moving heat source, utilizing the Moore-Gibson-Thompson (MGT) model with higher-order memory-dependent derivatives. Abouelregal *et al.* (2024) studied a modified nonlocal fractional magneto-thermoelastic model that includes higher-order time derivatives and phase-lags.

Lotfy (2012) studied the influence of reinforcement on the total deformation for an infinite space weakened by a finite linear opening mode-I crack. Abo-Dahab and Lotfy (2015) studied the generalized magneto-thermoelastic behavior of fiber-reinforced materials under rotational effects, incorporating fractional derivative heat transfer. Lotfy *et al.* (2019) examined the effects of variable thermal conductivity in a small semiconductor cavity using the fractional order heat-magneto-photothermal theory. Mahdy *et al.* (2021) studied focuses on developing numerical solutions and analyzing the dynamic behaviors of a fractional nonlinear Rubella disease model. Mahdy *et al.* (2021) focused on developing numerical methods to solve the Rubella ailment disease model. Lotfy *et al.* (2021) explored the interaction of piezoelectric, photothermal, and thermoelastic effects in semiconductor materials under the hyperbolic two-temperature theory. Lotfy and Tantawi (2020) discussed the interaction of photo-thermal-elastic waves in functionally graded materials (FGMs) under the influence of a magnetic field. Abo Dahab *et al.* (2015) investigated the effects of rotation and magnetic fields on the propagation of surface waves in an elastic layer over a generalized thermoelastic diffusive half-space with an imperfect boundary. Zenkour (2020) constructed the generalized photothermoelastic problem of beam with modified multi-phase-lag photothermoelasticity theory. Zakaria *et al.* (2021) used fractional calculus technique to construct a modified generalized fractional photothermeolastic model. Sharma and Kumar (2021) analysed deformation due to inclined loads in dynamic mathematical model of photothermoelastic (semiconductor) medium. Sharma and Kumar (2022) examined photothermoelastic deformation in dual phase lag model due to concentrated inclined load. Kumar *et al.* (2022) investigated deformation due to thermomechanical carrier density loading in orthotropic photothermoelastic plate. Kumar *et al.* (2022) studied the deformation due to thermomechanical and carrier density loading in orthotropic photothermoelastic plate under Moore-Gibson-Thompson thermoelastic model. Sharma and Khator (2021, 2022) examined some problems of power generation due to renewable sources.

It is well known that fractional calculus is still in infancy, although it has been invented for three centuries and applied widely in science and engineering. Also, memory-dependent derivative (MDD) preformed more detail examination of photothermoelastic deformation in continuum mechanics. The memory-dependent derivative of which time delay and kernel function can be chosen freely according to the necessity of application and found it is better than the fractional calculus for reflecting the memory effect was proposed by Wang and Li (2011). Yu *et al.* (2014) suggested a novel generalized thermoelasticity model based on MDD. (Ezzat *et al.* 2014, 2015, 2016) discussed some solutions of one-dimensional problems obtained with the use of the memory-dependent LS model of generalized thermoelasticity. Hendy *et al.* (2020) developed a generalized thermoelasticity model with memory-dependent derivative (MDD) heat conduction law for a thermoelastic half-space. Motivated by the above researchers the present work is an attempt to develop a new model of linear non-local photothermoelastic under hyperbolic two temperature, dual phase lag by incorporating the memory dependent derivative.

In this paper, deformation due to thermomechanical and carrier density loading in a new model of photothermoelasticity with memory-dependent derivatives (PMDD) under non-local (NL) parameter, dual phase lag (DPL) and hyperbolic two temperature (HTT) and has been investigated. Problem is simplified by integral transform technique (involving Laplace and Fourier transforms). In the new domain, physical field quantities (normal stress, conductive temperature field and carrier density distribution) are examined. By numerical inversion technique, convert the resulting expressions in the original physical domain. The variations of stress components, conductive temperature field and carrier density distribution are depicted graphically to demonstrate the effects of non-local parameter, DPL and HTT (with and without MDD) and the variation of all kernel functions due to normal force, thermal source and carrier density source are also presented. Some special cases are also introduced. Due to wide spread use of photothermoelastic nano material in a variety of field particularly in environment and catalytic applications.

2. Elementary equations

The governing equations for PMDD based on NL, DPL and HTT impacts by removing body forces, heat sources and carrier photogeneration sources are described by (Tazu 1995, Ezzat 2016)

$$t_{ij} = C_{ijkl}e_{kl} - \alpha_{ij}T - \gamma_{ij}N \tag{1}$$

$$C_{ijkl}e_{kl} - \alpha_{ij}T_{,h} - \gamma_{ij}N_{,h} = \rho(1-\xi_1^2\Delta)\ddot{u}_l \tag{2}$$

$$(1+\tau_T D_\omega)K_{ij}\varphi_{,ii} = \left(1+\tau_q D_\omega + \frac{\tau_q^2}{2!}D_\omega^2\right)\left[\left(\rho C_e\dot{T} + T_o\alpha_{ij}\dot{e}_{kk}\right) - \frac{E_g}{\tau}N\right] \tag{3}$$

$$D_{ij}^{*}N_{,ij} = \frac{\partial N}{\partial t} + \frac{N}{\tau} - \varepsilon\frac{T}{\tau} \tag{4}$$

$$\ddot{T} = \ddot{\varphi} - a_{ij}\varphi_{,jj} \quad (i, j, k, l = 1, 2, 3) \tag{5}$$

where

τ_T −phase lag of temperature gradient, τ_q −phase lag of heat flux, C_{ijkl} −elastic parameters, α_{ij} − coefficient of linear thermal expansion, γ_{ij} − coefficient of electronic deformation, u_i − components of displacement, T-temperature distribution, T_o − reference temperature, φ − conductive temperature $N = n - n_o$, n_o − equilibrium carrier concentration, E_g − semiconductor energy gap, ρ − medium density, t_{ij} − components of stress tensor, K_{ij} −thermal conductivity, C_e −specific heat, $\varepsilon = \frac{\partial n_o}{\partial T}$ the thermal activation coupling parameter, τ − photogenerated carrier lifetime, t-time variable, D_{ij}^{*} − coefficients of carrier diffusion, e_{kk} −components of elastic strain, ξ_1 −non-local parameter.

Diethelm (2010) has developed Caputo (1967) derivative to be

$$D_a^{\ell} f(t) = \int_a^t K_{\ell}(t-\xi)\, f^{(m)}(\xi) d\xi \tag{6}$$

with

$$K_{\ell}(t-\xi) = \frac{(t-\xi)^{m-\ell-1}}{\Gamma(m-\ell)} \tag{7}$$

where $K_{\ell}(t-\xi)$ is the kernel function and $f^{(m)}$ denotes the common m-order derivative, which has specific physical meaning.

Wang and Li (2011) introduced a memory-dependent derivative, the first order of function f which is simply defined in an integral form of a common derivative with a kernel function on a slipping interval, in the form

$$D_{\omega} f(t) = \frac{1}{\omega} \int_{t-\omega}^{t} K(t-\xi)\, f'(\xi) d\xi \tag{8}$$

where ω is the time delay and $K(t-\omega)$ is the kernel function in which they can be chosen freely.

$$K(t-\xi) = 1 - \frac{2n}{\omega}(t-\xi) + \frac{m^2(t-\xi)^2}{\omega^2} = \begin{cases} 1 if m = n = 0 \\ 1 - \frac{t-\xi}{\omega} if m = 0, n = 1/2 \\ 1 - (t-\xi) if m = 0, n = \omega/2, \\ \left(1 - \frac{(t-\xi)}{\omega}\right)^2 if m = 1, n = 1 \end{cases} \tag{8}$$

where m and n are constants.

Yu *et al*. (2014) introduced memory-dependent derivative into the Lord and Shulman (1967) generalized thermoelasticity theory. Ezzat *et al*. (2014) constructed a new generalized thermo-viscoelasticity theory with memory-dependent derivatives, to denote memory-dependence, as

$$q + \omega D_{\omega} q = -k \nabla T \tag{9}$$

Eq. (9) has more clear physical meaning.

The dynamic coupled theory of heat conduction law follows as the limit case when $\omega \to 0$, so that $|D_{\omega} f(x,t)| \leq \left|\frac{\partial f(x,t)}{\partial t}\right| = \left|\lim_{\omega \to 0} \frac{f(x,t+\omega) - f(x,t)}{\omega}\right|$

This model is more intuitionistic for understanding the physical meaning and the corresponding memory dependent differential equation is more expressive.

3. Formulation of the problem

An orthotropic PMDD half space based on NL, DPL and HTT impact ($x_3 \geq 0$) occupying the two-dimensional space has been taken for two dimensional problem in $x_1 - x_3$ plane. All the physical field variables are functions of x_1, x_3, t. Thus, the displacement components, temperature distribution and carrier density distribution are given by

$$u = \big(u_1(x_1, x_3, t), 0, u_3(x_1, x_3, t)\big), T = T(x_1, x_3, t) \text{ and } N = N(x_1, x_3, t) \tag{10}$$

We have used appropriate plane of symmetry, on the set of Eqs. (1)-(5) to derive the equations for orthotropic PMDD with NL, DPL and HTT parameter for two dimensional problem with the aid of Eq. (10), are reduced to following.

$$C_{11}\frac{\partial^2 u_1}{\partial x_1^2}+C_{55}\frac{\partial^2 u_1}{\partial x_3^2}+(C_{13}+C_{55})\frac{\partial^2 u_3}{\partial x_1\partial x_3}-\alpha_1\frac{\partial T}{\partial x_1}-\gamma_1\frac{\partial N}{\partial x_1}=\rho(1-\xi_1^2\Delta)\frac{\partial^2 u_1}{\partial t^2}, \tag{11}$$

$$C_{55}\frac{\partial^2 u_3}{\partial x_1^2}+C_{33}\frac{\partial^2 u_3}{\partial x_3^2}+(C_{13}+C_{55})\frac{\partial^2 u_1}{\partial x_1\partial x_3}-\alpha_3\frac{\partial T}{\partial x_3}-\gamma_3\frac{\partial N}{\partial x_3}=\rho(1-\xi_1^2\Delta)\frac{\partial^2 u_3}{\partial t^2}, \tag{12}$$

$$(1+\tau_T D_\omega)\left(K_1\frac{\partial^2\varphi}{\partial x_1^2}+K_3\frac{\partial^2\varphi}{\partial x_3^2}\right)=\left(1+\tau_q D_\omega+\frac{\tau_q^2}{2!}D_\omega^2\right)$$
$$\left[\left(\rho C_e\frac{\partial T}{\partial t}+T_o\left(\alpha_1\frac{\partial^2 u_1}{\partial x_1\partial t}+\alpha_3\frac{\partial^2 u_3}{\partial x_3\partial t}\right)-\frac{E_g}{\tau}N\right)\right], \tag{13}$$

$$D_1^*\frac{\partial^2 N}{\partial x_1^2}+D_3^*\frac{\partial^2 N}{\partial x_3^2}=\frac{\partial N}{\partial t}+\frac{N}{\tau}-\varepsilon\frac{T}{\tau}, \tag{14}$$

$$t_{33}=C_{13}\frac{\partial u_1}{\partial x_1}+C_{33}\frac{\partial u_3}{\partial x_3}-\alpha_3 T-\gamma_3 N, \tag{15}$$

$$t_{31}=C_{55}\left(\frac{\partial u_1}{\partial x_3}+\frac{\partial u_3}{\partial x_1}\right), \tag{16}$$

$$\frac{\partial^2 T}{\partial t^2}=\frac{\partial^2\varphi}{\partial t^2}-\left(a_1\frac{\partial^2}{\partial x_1^2}+a_3\frac{\partial^2}{\partial x_3^2}\right)\varphi, \tag{17}$$

where

$$\alpha_1=C_{11}\alpha_1^*+C_{12}\alpha_2^*+C_{13}\alpha_3^*,\ \alpha_3=C_{13}\alpha_1^*+C_{23}\alpha_2^*+C_{33}\alpha_3^*$$
$$\gamma_1=C_{11}\gamma_1^*+C_{12}\gamma_2^*+C_{13}\gamma_3^*,\ \gamma_3=C_{13}\gamma_1^*+C_{23}\gamma_2^*+C_{33}\gamma_3^* \tag{18}$$

α_1^*,α_2^* and α_3^* are linear thermal expansion coefficients, γ_1^*,γ_2^* and $\gamma_3^*$are electronic deformation coefficients, K_1,K_3 are thermal conductivity, D_1^* and D_3^* are carrier diffusion coefficients.

In the above equations we use the contracting subscript notations ($11\to 1, 22\to 2{,}33\to 3{,}23\to 4{,}31\to 5{,}12\to 6$) to relate C_{ijkl} to C_{mn}.

Also

$$K_{ij}\delta_{ij}=K_i \text{ and } D_{ij}^*\delta_{ij}=D_i^*, i \text{ is not summed.}$$

For non-dimensionalization of equations, following variables are taken

$$(x_1',x_3',u_1',u_3')=\eta_1 C_o(x_1,x_3,u_1,u_3)\ ,(t_{11}',t_{33}',t_{31}')=\frac{1}{C_{11}}(t_{11},t_{33},t_{31}),$$
$$(t',\tau_o',\tau')=\eta_1 C_o^2(t,\tau_o,\tau), T'=\frac{\alpha_1 T}{\rho C_o^2}, \phi'=\frac{\alpha_1\phi}{\rho C_o^2}, N'=\frac{N}{n_o}, \xi_1{}'=\frac{\xi_1}{(\eta_1 C_o)^2}, (a_1',a_3')=\frac{(a_1,a_3)}{C_o^2} \tag{19}$$

also

$$\eta_1=\frac{\rho C_e}{K_1}, C_o^2=\frac{C_{11}}{\rho}.$$

Eqs. (11)-(17) reduce to the following form by taking into consideration Eq. (19) and after suppressing the prime as

$$\frac{\partial^2 u_1}{\partial x_1^2}+g_1\frac{\partial^2 u_1}{\partial x_3^2}+g_2\frac{\partial^2 u_3}{\partial x_1\partial x_3}-\frac{\partial T}{\partial x_1}-g_3\frac{\partial N}{\partial x_1}=(1-\xi_1^2\Delta)\frac{\partial^2 u_1}{\partial t^2}, \tag{20}$$

$$\frac{\partial^2 u_3}{\partial x_1^2}+g_4\frac{\partial^2 u_3}{\partial x_3^2}+g_5\frac{\partial^2 u_1}{\partial x_1\partial x_3}-g_6\frac{\partial T}{\partial x_3}-g_7\frac{\partial N}{\partial x_3}=g_8(1-\xi_1^2\Delta)\frac{\partial^2 u_3}{\partial t^2}, \tag{21}$$

$$(1+\tau_T D_\tau)\left(\frac{\partial^2\varphi}{\partial x_1^2}+K^*\frac{\partial^2\varphi}{\partial x_3^2}\right)=\left(1+\tau_q D_\tau+\frac{\tau_q^2}{2!}D_\tau^2\right)\left[\left(\frac{\partial T}{\partial t}+g_9\frac{\partial}{\partial t}\left(\frac{\partial u_1}{\partial x_1}+\alpha^*\frac{\partial u_3}{\partial x_3}\right)-g_{10}\frac{N}{\tau}\right)\right], \tag{22}$$

$$\frac{\partial^2 N}{\partial x_1^2} + D^* \frac{\partial^2 N}{\partial x_3^2} = g_{11} \frac{\partial N}{\partial t} + g_{11} \frac{N}{\tau} - g_{12} \frac{T}{\tau}, \tag{23}$$

$$t_{33} = g_{13} \frac{\partial u_1}{\partial x_1} + g_{14} \frac{\partial u_3}{\partial x_3} - g_{15} T - g_{16} N, \tag{24}$$

$$t_{31} = g_1 \left(\frac{\partial u_1}{\partial x_3} + \frac{\partial u_3}{\partial x_1} \right), \tag{25}$$

$$\frac{\partial^2 T}{\partial t^2} = \frac{\partial^2 \varphi}{\partial t^2} - \left(a_1 \frac{\partial^2 \varphi}{\partial x_1^2} + a_3 \frac{\partial^2 \varphi}{\partial x_3^2} \right). \tag{26}$$

where

$$g_1 = \frac{C_{55}}{C_{11}}, g_2 = \frac{C_{13}+C_{55}}{C_{11}}, g_3 = \frac{\gamma_1 n_o}{C_{11}}, g_4 = \frac{C_{33}}{C_{55}}, g_5 = \frac{C_{13}+C_{55}}{C_{55}}, g_6 = \frac{\alpha_3 C_{11}}{\alpha_1 C_{55}}, g_7 = \frac{\gamma_3 n_o}{C_{55}},$$
$$g_8 = \frac{1}{C_{55}}, g_9 = \frac{T_o \alpha_1 \alpha_1}{\rho^2 C_e C_o^2}, g_{10} = \frac{E_g n_o \alpha_1}{\rho^2 C_e C_o^2}, g_{11} = \frac{1}{\eta_1 D_1^*}, g_{12} = \frac{\varepsilon C_{11}}{\alpha_1 D_1^* n_o \eta_1}, g_{13} = \frac{C_{13}}{C_{11}}, g_{14} = \frac{C_{33}}{C_{11}},$$
$$g_{15} = \frac{\alpha_3}{\alpha_1}, g_{16} = \frac{\gamma_3 n_o}{C_{11}}, K^* = \frac{K_3}{K_1}, D^* = \frac{D_3^*}{D_1^*}, \alpha^* = \frac{\alpha_3}{\alpha_1}. \tag{27}$$

Define Laplace and Fourier Transform as

$$\overline{f}(x_1, x_{3,} p) = \int_0^\infty f(x_1, x_{3,} p)\, e^{-pt} dt, \tag{28}$$

$$\hat{f}(\zeta, x_{3,} p) = \int_{-\infty}^\infty \bar{f}\,(x_1, x_{3,} p) e^{i\zeta x_1} dx_1. \tag{29}$$

Applying Laplace and Fourier transforms defined by (28)-(29) on Eqs. (20)-(26), the following equations are obtained

$$\left(g_{17} \frac{d^2}{dx_3^2} + g_{18} \right) \hat{u}_1 + g_{19} \frac{d\hat{u}_3}{dx_3} - \left(g_{20} \frac{d^2}{dx_3^2} + g_{21} \right) \hat{\varphi} + g_{22} \widehat{N} = 0, \tag{30}$$

$$\left(g_{23} \frac{d\hat{u}_1}{dx_3} \right) + \left(g_{24} \frac{d^2}{dx_3^2} + g_{25} \right) \hat{u}_3 - \left(g_{26} \frac{d}{dx_3} + g_{27} \frac{d^3}{dx_3^3} \right) \hat{\varphi} - g_7 \frac{d\widehat{N}}{dx_3} = 0, \tag{31}$$

$$\left(g_{29} \frac{d^2}{dx_3^2} + g_{30} \right) \hat{\varphi} + \left(\frac{d^2}{dx_3^2} + g_{28} \right) \widehat{N} = 0, \tag{32}$$

$$g_{31} \hat{u}_1 + g_{32} \frac{d\hat{u}_3}{dx_3} - \left(g_{33} \frac{d^2}{dx_3^2} + g_{34} \right) \hat{\varphi} - g_{35} \widehat{N} = 0, \tag{33}$$

$$\hat{t}_{33} = -g_{13} i\zeta \hat{u}_1 + g_{14} \frac{d\hat{u}_3}{dx_3} - g_{15} \left(1 - \varepsilon_1^2 \left(-\zeta^2 + a * \frac{d^2}{dx_3^2} \right) \right) \hat{\varphi} - g_{16} \widehat{N}, \tag{34}$$

$$\hat{t}_{31} = g_1 \left(\frac{d\hat{u}_1}{dx_3} - i\zeta \hat{u}_3 \right), \tag{35}$$

also

$$g_{17} = -p^2 \xi_1^2 + g_1, g_{18} = -\zeta^2 - p^2(1 + \zeta^2 \xi_1^2),$$
$$g_{19} = i\zeta g_2, g_{20} = i\zeta \varepsilon_1^2 a^*, g_{21} = i\zeta + i\zeta^3 \varepsilon_1^2,$$
$$g_{22} = -i\zeta g_3, g_{23} = i\zeta g_5, g_{24} = g_4 + g_8 p^2 \xi_1^2,$$
$$g_{25} = -\zeta^2 - g_8 p^2 (1 + \zeta^2 \xi_1^2), g_{26} = g_6 (1 + \zeta^2 \varepsilon_1^2),$$
$$g_{27} = g_6 a^* \varepsilon_1^2,\ g_{28} = \frac{1}{D^*} \left(\zeta^2 - g_9 p - \frac{g_9}{\tau} \right),$$
$$g_{29} = -\frac{g_{10}}{\tau} \varepsilon_1^2 a^*,\ g_{30} = \frac{g_{10}}{\tau} (1 + \varepsilon_1^2 \zeta^2),$$

$$g_{31} = -i\zeta p g_{11} G_2,\ g_{32} = -g_{11} p a^* G_2,$$
$$g_{33} = K^* G_1 + \varepsilon_1^2 a^* G_2,$$
$$g_{34} = -G_1 \zeta^2 - G_2 p(1 + \varepsilon_1^2 \zeta^2 + \varepsilon_1^2 a^*),\ g_{35} = \frac{G_2 g_{12}}{\tau},$$
$$G_1 = \left(1 + \frac{\tau_T}{\omega} G(p,\omega)\right), G_2 = \left(1 + \frac{\tau_q}{\omega} G(p,\omega) + \frac{\tau_q^2}{2\omega} G(p,\omega)\right). \tag{36}$$

where Laplace transform of memory dependent derivative is

$$L\{D_\omega f(t)\} = L\left\{\int_{t-\omega}^{t} K(t-\xi)\, f'(\xi) d\xi\right\} = F(s).\, G(p,\omega),$$
$$G(p,\omega) = (1 - e^{-p\omega})\left(1 - \frac{2n}{\omega p} + \frac{2m^2}{\omega^2 p^2}\right) - \left(m^2 - 2n + \frac{2m^2}{\omega p}\right) e^{-p\omega}, \tag{37}$$

m and *n* are constants such that

$$F(s) = L\left\{\left(\frac{\partial T}{\partial t} + g_9 \frac{\partial}{\partial t}\left(\frac{\partial u_1}{\partial x_1} + \alpha^* \frac{\partial u_3}{\partial x_3}\right) - g_{10} \frac{N}{\tau}\right)\right\}, \tag{38}$$

After some algebraic calculation of Eqs. (30) - (33), determine the following

$$(R_1 D^8 + R_2 D^6 + R_3 D^4 + R_4 D^2 + R_5)\left(\hat{u}_1, \hat{u}_3, \hat{\varphi}, \widehat{N}\right) = 0. \tag{39}$$

where

$$R_1 = g_{17} g_{24} g_{33} - g_{17} g_{27} g_{24},$$
$$R_2 = g_{17} g_{24} g_{34} + g_{17} g_{25} g_{33} - g_{17} g_{26} g_{32} + g_{18} g_{24} g_{33}$$
$$- g_{19} g_{23} g_{33} + g_{20} g_{23} g_{32} - g_{20} g_{24} g_{31} - g_{18} g_{27} g_{32}$$
$$- g_7 g_{17} g_{29} g_{32} - g_{17} g_{24} g_{28} g_{33} + g_{17} g_{27} g_{28} g_{32}$$
$$- g_{17} g_{24} g_{29} g_{35},$$
$$R_3 = g_{17} g_{25} g_{34} + g_{18} g_{24} g_{34} + g_{18} g_{25} g_{33} - g_{18} g_{26} g_{32}$$
$$- g_{19} g_{23} g_{34} + g_{19} g_{26} g_{31} - g_{20} g_{25} g_{31} + g_{21} g_{23} g_{32}$$
$$- g_{21} g_{24} g_{31} - g_7 g_{17} g_{30} g_{32} - g_7 g_{18} g_{29} g_{32} - g_7 g_{19} g_{29} g_{31}$$
$$- g_{17} g_{24} g_{28} g_{34} - g_{17} g_{25} g_{28} g_{33} + g_{17} g_{26} g_{28} g_{32}$$
$$- g_{18} g_{24} g_{28} g_{33} + g_{19} g_{23} g_{28} g_{33} - g_{20} g_{23} g_{28} g_{32} +$$
$$g_{18} g_{27} g_{28} g_{32} - g_{19} g_{27} g_{28} g_{31} - g_{17} g_{24} g_{30} g_{35}$$
$$- g_{17} g_{25} g_{29} g_{35} - g_{18} g_{24} g_{29} g_{35} + g_{19} g_{23} g_{29} g_{35}$$
$$- g_{22} g_{23} g_{29} g_{32} + g_{22} g_{24} g_{29} g_{31},$$
$$R_4 = g_{18} g_{25} g_{34} - g_{21} g_{25} g_{31} - g_7 g_{18} g_{30} g_{32} +$$
$$g_7 g_{19} g_{30} g_{31} - g_{17} g_{25} g_{28} g_{34} - g_{18} g_{24} g_{28} g_{26} -$$
$$g_{18} g_{25} g_{28} g_{33} + g_{18} g_{26} g_{28} g_{32} + g_{19} g_{23} g_{28} g_{34} -$$
$$g_{19} g_{26} g_{28} g_{31} + g_{20} g_{25} g_{28} g_{31} - g_{21} g_{23} g_{28} g_{32} +$$
$$g_{21} g_{24} g_{28} g_{31} - g_{17} g_{25} g_{30} g_{35} - g_{18} g_{24} g_{30} g_{35} -$$

$$
\begin{aligned}
&g_{18}g_{25}g_{29}g_{35}+g_{19}g_{23}g_{30}g_{35}-g_{22}g_{23}g_{30}g_{32}+\\
&g_{22}g_{24}g_{30}g_{31}+g_{22}g_{25}g_{30}g_{31},\\
&R_5=g_{18}g_{25}g_{34}g_{28}-g_{21}g_{25}g_{30}g_{31}-g_{18}g_{25}g_{30}g_{35}\\
&+g_{22}g_{25}g_{30}g_{31},
\end{aligned}
\tag{40}
$$

The general solution of Eq. (39) is written as

$$\left(\hat{u}_1,\hat{u}_3,\hat{\varphi},\widehat{N}\right)=\sum_{j=1}^{4}\left(1,h_{1j},h_{2j},h_{3j}\right)C_j e^{-m_j x_3}. \tag{41}$$

where $m_j(j=1,2,3,4)$ are roots of $(R_1D^8+R_2D^6+R_3D^4+R_4D^2+R_5)$ and coupling parameters are

$$h_{1j}=\sum_{j=1}^{4}\frac{R_{10}m_j^5+R_{11}m_j^3+R_{12}m_j}{R_6m_j^6+R_7m_j^4+R_8m_j^2+R_9}, \tag{42}$$

$$h_{2j}=\sum_{j=1}^{4}\frac{R_{13}m_j^4+R_{14}m_j^2+R_{15}}{R_6m_j^6+R_7m_j^4+R_8m_j^2+R_9}, \tag{43}$$

$$h_{3j}=\sum_{j=1}^{4}\frac{R_{16}m_j^4+R_{17}m_j^2+R_{18}}{R_6m_j^6+R_7m_j^4+R_8m_j^2+R_9}. \tag{44}$$

where

$$
\begin{gathered}
R_6=g_{24}g_{33}-g_{27}g_{32},\\
R_7=g_{24}g_{34}+g_{25}g_{33}-g_{26}g_{32}-g_7g_{29}g_{32}-\\
g_{24}g_{28}g_{33}+g_{27}g_{28}g_{32}-g_{24}g_{29}g_{35},\\
R_8=g_{25}g_{34}-g_7g_{30}g_{32}-g_{24}g_{28}g_{34}-g_{25}g_{28}g_{31}\\
+g_{26}g_{28}g_{32}-g_{24}g_{30}g_{35}-g_{25}g_{29}g_{35},\\
R_9=-g_{25}g_{30}g_{35}-g_{25}g_{28}g_{34},\ R_{10}=g_{27}g_{31}-g_{23}g_{33},\\
R_{11}=g_{26}g_{31}-g_{23}g_{34}+g_7g_{29}g_{31}-g_{23}g_{28}g_{33}-\\
g_{27}g_{28}g_{33}+g_{23}g_{29}g_{35},\\
R_{12}=g_7g_{30}g_{31}+g_{28}g_{23}g_{27}-g_{28}g_{26}g_{31}+g_{23}g_{30}g_{35},\\
R_{13}=g_{23}g_{32}-g_{24}g_{31},\ R_{14}=g_{24}g_{28}g_{31}-g_{23}g_{28}g_{32}-g_{25}g_{31},\ R_{15}=g_{25}g_{28}g_{31},\\
R_{16}=g_{23}g_{29}g_{32}-g_{24}g_{29}g_{31},\ R_{17}=g_{23}g_{30}g_{32}-g_{24}g_{30}g_{31}-g_{25}g_{29}g_{31},\\
R_{18}=g_{25}g_{30}g_{31},
\end{gathered}
\tag{45}
$$

Expressions for stress components are obtained with the aid of (31), (32) and (38) as

$$
\begin{aligned}
\hat{t}_{33}=&-i\zeta g_{13}\sum_{j=1}^{4}C_je^{-m_jx_3}-g_{14}\sum_{j=1}^{4}h_{1j}m_jC_je^{-m_jx_3}\\
&-g_{15}\left[\left(1-\varepsilon_1^2\left(-\zeta^2+a*\frac{d^2}{dx_3^2}\right)\right)\right]\sum_{j=1}^{4}h_{2j}C_je^{-m_jx_3}-g_{16}\sum_{j=1}^{4}h_{3j}C_je^{-m_jx_3},
\end{aligned}
\tag{46}
$$

$$\hat{t}_{31}=-g_1\sum_{j=1}^{4}m_jC_je^{-m_jx_3}-i\zeta g_1\sum_{j=1}^{4}h_{1j}C_je^{-m_jx_3}. \tag{47}$$

4. Restrictions on the boundary

The boundary restrictions for the assumed model are subjected to exponential decaying normal force, thermal source distributed over the plane $x_1 = 0$ and carrier density source moving with the positive direction of x_1, at the plane $x_3 = 0$ are considered as

$$\left.\begin{array}{l} t_{33} = -F_1(x_1, t), \\ t_{31} = 0, \\ \varphi = F_2(x_1, t), \\ N = F_3(x_1, t), \end{array}\right\} \text{at } x_3 = 0 \tag{48}$$

where

$$F_1(x_1, t) = \frac{F_{10}}{16}\frac{t^2}{t_p^2} e^{-\frac{t}{t_p}} H(a - |x_1|), \tag{49}$$

$$F_2(x_1, t) = \delta(x_1)\begin{cases} F_{20}\dfrac{\sin \pi t}{\eta}; 0 \le t \le \eta \\ 0, t > \eta \end{cases} \tag{50}$$

$$F_3(x_1, t) = F_{30}\delta(x_1 - \upsilon t). \tag{51}$$

also, $H\,(\,)$ is Heaviside step function, $\delta(\,)$ is Dirac delta function, v is the velocity, F_{10} is the magnitude of the force, F_{20} is the constant temperature applied on the boundary and F_{30} is constant.

Applying Laplace and Fourier transform defined by Eqs. (28)-(29) on Eqs. (48)-(51), we attain

$$\left.\begin{array}{l} \hat{t}_{33} = -\hat{F}_1(\zeta, p) = -\frac{F_{10}}{8}\frac{t_p}{(1+pt_p)^3}\frac{\sin a\zeta}{\zeta}, \\ \hat{t}_{31} = 0, \\ \hat{\varphi} = \hat{F}_2(\zeta, p) = F_{20}\frac{\pi\eta}{\pi^2+\eta^2 p^2}(1 + e^{-p\eta}),, \\ \hat{N} = \hat{F}_3(\zeta, p) = \frac{F_{30}}{\upsilon} e^{-\frac{p}{\upsilon}x_1}, \end{array}\right\} \text{at } x_3 = 0 \tag{52}$$

Substituting the values of $\hat{t}_{33}, \hat{t}_{31}, \hat{\varphi}$ and $\hat{N}$ from Eqs. (41), (46) and (47) in the transformed boundary restrictions (52), determine the arbitrary constants which on substituting in the resulting Eqs. (41), (46) and (47) yield the displacement components, stress components, conductive temperature and carrier density distribution as

$$\hat{u}_1 = \frac{1}{\Delta}\left(L_1\hat{F}_1(\zeta, p) + L_2\hat{F}_2(\zeta, p) + L_3\hat{F}_3(\zeta, p)\right), \tag{53}$$

$$\hat{u}_3 = \frac{1}{\Delta}\left(L_4\hat{F}_1(\zeta, p) + L_5\hat{F}_2(\zeta, p) + L_6\hat{F}_3(\zeta, p)\right), \tag{54}$$

$$\hat{t}_{33} = \frac{1}{\Delta}\left(L_7\hat{F}_1(\zeta, p) + L_8\hat{F}_2(\zeta, p) + L_9\hat{F}_3(\zeta, p)\right), \tag{55}$$

$$\hat{t}_{31} = \frac{1}{\Delta}\left(L_{10}\hat{F}_1(\zeta, p) + L_{11}\hat{F}_2(\zeta, p) + L_{12}\hat{F}_3(\zeta, p)\right), \tag{56}$$

$$\hat{\varphi} = \frac{1}{\Delta}\left(L_{13}\hat{F}_1(\zeta, p) + L_{14}\hat{F}_2(\zeta, p) + L_{15}\hat{F}_3(\zeta, p)\right), \tag{57}$$

$$\hat{N} = \frac{1}{\Delta}\left(L_{16}\hat{F}_1(\zeta, p) + L_{17}\hat{F}_2(\zeta, p) + L_{18}\hat{F}_3(\zeta, p)\right). \tag{58}$$

where

$$
\begin{aligned}
&E=e^{-(m_1+m_2+m_3+m_4)x_3}\\
&(L_1,L_2,L_3)=E\begin{bmatrix}(R_{17}+R_{20}+R_{23}+R_{26}),\\ (R_{18}+R_{21}+R_{24}+R_{27}),(R_{19}+R_{22}+R_{25}+R_{28})\end{bmatrix},\\
&(L_4,L_5)=E\begin{bmatrix}(R_{17}h_{11}+R_{20}h_{12}+R_{23}h_{13}+R_{26}h_{14}),\\ (R_{18}h_{11}+R_{21}h_{12}+R_{24}h_{13}+R_{27}h_{14})\end{bmatrix}\\
&(L_6,L_7)=E\begin{bmatrix}(R_{19}h_{11}+R_{22}h_{12}+R_{25}h_{13}+R_{28}h_{14}),\\ (R_{17}d_{11}+R_{20}d_{21}+R_{23}d_{31}+R_{26}d_{41})\end{bmatrix}\\
&(L_8,L_9)=E\begin{bmatrix}(R_{18}d_{11}+R_{21}d_{21}+R_{24}d_{31}+R_{27}d_{41}),\\ (R_{19}d_{11}+R_{22}d_{21}+R_{25}d_{31}+R_{28}d_{41})\end{bmatrix}\\
&(L_{10},L_{11})=E\begin{bmatrix}(R_{17}d_{12}+R_{20}d_{22}+R_{23}d_{32}+R_{26}d_{42}),\\ (R_{18}d_{12}+R_{21}d_{22}+R_{24}d_{32}+R_{27}d_{42})\end{bmatrix}\\
&(L_{12},L_{13})=E\begin{bmatrix}(R_{19}d_{12}+R_{22}d_{22}+R_{25}d_{32}+R_{28}d_{42}),\\ (R_{17}h_{21}+R_{20}h_{22}+R_{23}h_{23}+R_{26}h_{24})\end{bmatrix}\\
&(L_{14},L_{15})=E\begin{bmatrix}(R_{18}h_{21}+R_{21}h_{22}+R_{24}h_{23}+R_{27}h_{24}),\\ (R_{19}h_{21}+R_{22}h_{22}+R_{25}h_{23}+R_{28}h_{24})\end{bmatrix}\\
&(L_{16},L_{17},L_{18})=E\begin{bmatrix}(R_{17}h_{31}+R_{20}h_{32}+R_{23}h_{33}+R_{26}h_{34}),\\ (R_{18}h_{31}+R_{21}h_{32}+R_{24}h_{33}+R_{27}h_{34})\\ ,(R_{19}h_{31}+R_{22}h_{32}+R_{25}h_{33}+R_{28}h_{34})\end{bmatrix}
\end{aligned}
\tag{59}
$$

also

$$
\begin{aligned}
d_{j1}&=-i\zeta g_{13}-m_j g_{14}h_{1j}-g_{15}h_{3j}\\
&\quad\left(1-\varepsilon_1^2\left(-\zeta^2+a*m_j^2\right)\right)-g_{16}h_{3j}\\
d_{j2}&=-i\zeta g_1 h_{1j}-m_j g_1\ (j=1,2,3,4).
\end{aligned}
$$

$$
\begin{aligned}
R_{17}&=d_{22}h_{23}h_{34}-d_{22}h_{24}h_{33}-d_{32}h_{22}h_{34}+d_{32}h_{24}h_{32}\\
&+d_{42}h_{22}h_{33}-d_{42}h_{23}h_{32},\\
R_{18}&=d_{21}d_{32}h_{34}-d_{22}d_{31}h_{34}-d_{21}d_{42}h_{33}+d_{22}d_{41}h_{33}\\
&+d_{31}d_{42}h_{32}-d_{32}d_{41}h_{32},\\
R_{19}&=d_{22}d_{31}h_{24}-d_{21}d_{32}h_{24}+d_{21}d_{42}h_{23}-d_{22}d_{41}h_{23}\\
&-d_{31}d_{42}h_{22}+d_{32}d_{41}h_{22},\\
R_{20}&=-d_{12}h_{23}h_{34}+d_{12}h_{24}h_{33}+d_{32}h_{21}h_{34}-d_{32}h_{24}h_{31}\\
&-d_{42}h_{21}h_{33}+d_{42}h_{23}h_{31},\\
R_{21}&=-d_{11}d_{32}h_{34}+d_{12}d_{31}h_{34}+d_{11}d_{42}h_{33}-d_{12}d_{41}h_{33}\\
&-d_{31}d_{42}h_{31}+d_{32}d_{41}h_{31},
\end{aligned}
$$

$$
\begin{aligned}
&R_{22}=d_{11}d_{32}h_{24}-d_{12}d_{31}h_{24}-d_{11}d_{42}h_{23}+d_{12}d_{41}h_{23}\\
&+d_{31}d_{42}h_{21}-d_{32}d_{41}h_{21},\\
&R_{23}=d_{12}h_{22}h_{34}-d_{12}h_{24}h_{32}-d_{22}h_{21}h_{34}+d_{22}h_{24}h_{31}\\
&+d_{42}h_{21}h_{32}-d_{42}h_{22}h_{31},\\
&R_{24}=d_{11}d_{22}h_{34}-d_{12}d_{21}h_{34}-d_{11}d_{42}h_{32}+d_{12}d_{41}h_{32}\\
&+d_{21}d_{42}h_{11}-d_{22}d_{41}h_{31},\\
&R_{25}=d_{12}d_{21}h_{24}-d_{11}d_{22}h_{24}+d_{11}d_{42}h_{22}-d_{12}d_{41}h_{22}\\
&+d_{21}d_{42}h_{21}-d_{22}d_{41}h_{21},\\
&R_{26}=d_{12}h_{22}h_{33}+d_{12}h_{23}h_{32}+d_{22}h_{21}h_{33}-d_{22}h_{23}h_{31}-\\
&d_{32}h_{21}h_{32}+d_{32}h_{22}h_{31},\\
&R_{27}=d_{11}d_{22}h_{33}+d_{12}d_{21}h_{33}-d_{11}d_{32}h_{32}+d_{12}d_{31}h_{32}\\
&+d_{21}d_{32}h_{31}+d_{22}d_{31}h_{31},\\
&R_{28}=d_{11}d_{22}h_{23}-d_{12}d_{21}h_{23}-d_{11}d_{32}h_{22}-d_{12}d_{31}h_{22}+\\
&d_{21}d_{32}h_{21}-d_{22}d_{31}h_{21},
\end{aligned}
\tag{60}
$$

5. Particular cases

(i) For moving normal force $F_{20}=F_{30}=0$ yield

$$\left(\hat{u}_1,\hat{u}_3,\hat{t}_{33},\hat{t}_{31},\hat{\varphi},\hat{N}\right)=\frac{1}{\Delta}\Big((L_1,L_4,L_7,L_{10},L_{13},L_{16})\hat{F}_1(\zeta,p)\Big), \tag{61}$$

where $\hat{F}_1(\zeta,p)$ is given by Eq. (52).

(ii) For ramp type thermal Source $F_{10}=F_{30}=0$ yield

$$\left(\hat{u}_1,\hat{u}_3,\hat{t}_{33},\hat{t}_{31},\hat{\varphi},\hat{N}\right)=\frac{1}{\Delta}\Big((L_2,L_5,L_8,L_{11},L_{14},L_{17})\hat{F}_2(\zeta,p)\Big), \tag{62}$$

where $\hat{F}_2(\zeta,p)$ is given by Eq. (52).

(iii) For carrier density source $F_{10}=F_{20}=0$ yield

$$\left(\hat{u}_1,\hat{u}_3,\hat{t}_{33},\hat{t}_{31},\hat{\varphi},\hat{N}\right)=\frac{1}{\Delta}\Big((L_3,L_6,L_9,L_{12},L_{15},L_{18})\hat{F}_3(\zeta,p)\Big), \tag{63}$$

where $\hat{F}_3(\zeta,p)$ is given by Eq. (52).

6. Unique cases

a) $If\, C_{11}=C_{33}=\lambda+2\mu, C_{13}=\lambda, C_{55}=\mu, \alpha_{1t}=\alpha_{3t}=\alpha_t, \gamma_{1d}=\gamma_{3d}=\gamma_n, D_1=D_3=D_e$ and $K_1=K_3=K$ in Eqs. (53)-(58), then all corresponding results are obtained for isotropic photothermoelastic half space based on MDD under NL, DPL and HTT parameters.

b) In absence of (τ=0) in Eqs. (53)-(58), we obtain the corresponding expressions of $\hat{u}_1,\hat{u}_3$ and $\hat{\varphi}$ for half space based on orthotropic MDD under NL, DPL and HTT parameter, as where m_1, m_2, m_3 be the roots of characteristic equation.

$$D^6 + R_{29}D^4 + R_{30}D^2 + R_{31} = 0,\ (\hat{u}_1, \hat{u}_3, \hat{\varphi}) = \sum_{j=1}^{3}\left(1, r_j, s_j\right) C_j e^{-m_j x_3},$$

The coupling parameters are as

$$r_j = \sum_{j=1}^{3} \frac{R_{35}m_j^3 + R_{36}m_j}{R_{32}m_j^4 + R_{33}m_j^2 + R_{34}},\ \text{and}\ s_j = \sum_{j=1}^{3} \frac{R_{37}m_j^2 + R_{38}}{R_{32}m_j^4 + R_{33}m_j^2 + R_{34}}.$$

7. Inversion of transformation

To obtain the normal stress, temperature distribution and carrier density distribution in physical domain, we invert the Laplace and Fourier transforms by using the method given by Honig and Hirdes (1984).

8. Numerical results and discussion

For the numerical calculations, we take material constants for orthotropic Silicon (Si) material as

$$C_{11} = 19.45\,\mathrm{N/m^2},\ C_{13} = 6.41\,\mathrm{N/m^2},\ C_{33} = 16.57\,\mathrm{N/m^2},\ C_{55} = 7.96\,\mathrm{N/m^2},$$
$$\alpha_{1t} = 3.25\,\mathrm{N/m^2K},\ \alpha_{3t} = 3.10\,\mathrm{N/m^2K},\ \gamma_{1d} = -0.029715\,\mathrm{m^3},\ \gamma_{3d} = -0.02714\,\mathrm{m^3},$$
$$\rho = 2328\,\mathrm{kg/m^3},\ T_o = 300\,\mathrm{K},\ T_p = 2\,\mathrm{ps},\ K_1 = 150\,\mathrm{w/mk},\ K_3 = 152\,\mathrm{w/mk},\ E_g = 1.11\,eV,$$
$$C_e = 710\,\mathrm{j/kg\,K},\ \tau = 5\,\mathrm{s},\ \xi = 0.005,\ a_1 = 0.7,\ a_3 = 0.8,\ D_1^* = 4.0\,\mathrm{m^2/s},\ D_3^* = 3.5\,\mathrm{m^2/s},$$
$$n_o = 10^{20}\,\mathrm{m^{-3}}.$$

Case-I: Figs. 1.1-1.9 depict the variations of all field variables with distance x_1 on the plane $x_3 = 1$ for the different values of kernel.

Figs. 1.1-1.3 represent normal force (NF), Figs. 1.4-1.6 represents thermal source (TS), Figs. 1.7-1.9 represent carrier density source (CDS). In all the Figs. solid line correspond to $K(t,\xi) = 1 if m = n = 0(Kernel - 1)$, dashed line corresponds to

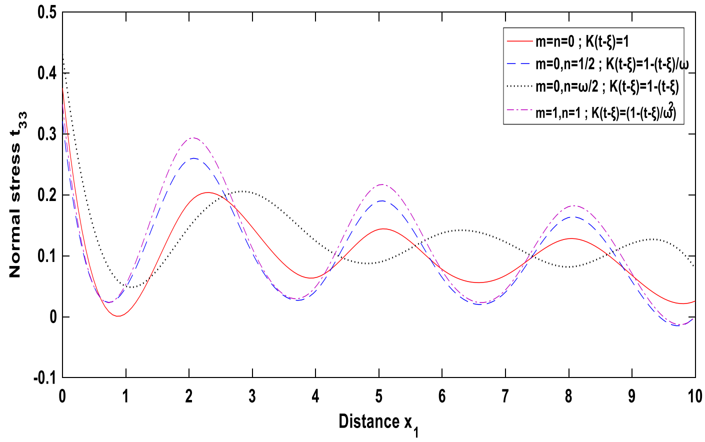

Fig. 1.1 Profile of t_{33} vs x_1 (NF with different values of kernel)

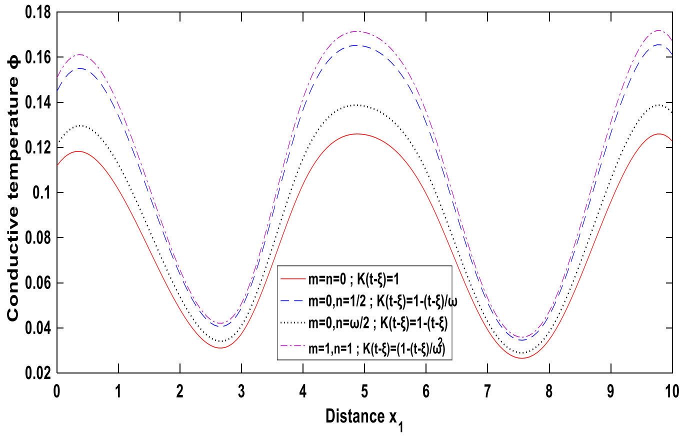

Fig. 1.2 Profile of ϕ vs x_1 (NF with different values of kernel)

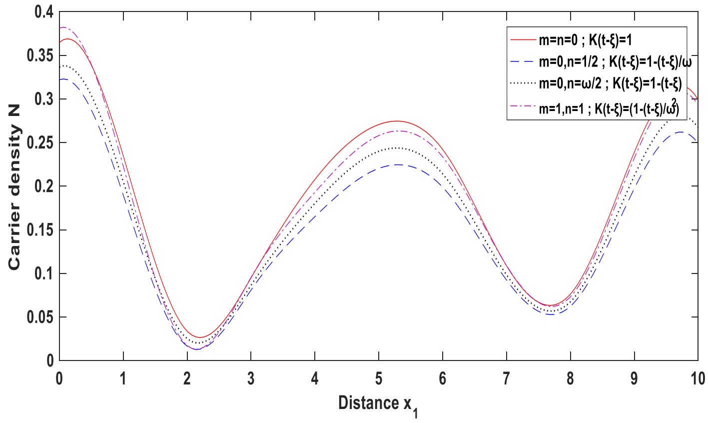

Fig. 1.3 Profile of N vs x_1 (NF with different values of kernel)

$$K(t,\xi) = 1 - \frac{t-\xi}{\omega} if m = 0, n = 1/2 (Kernel - 2),$$

dotted line corresponds to
$K(t,\xi) = 1 - (t - \xi) if m = 0, n = \omega/2 (Kernel - 3)$ and dash-dot line corresponds to

$$K(t,\xi) = \left(1 - \frac{t-\xi}{\omega}\right)^2 if m = n = 1 (Kernel - 4).$$

Figs. 1.1-1.3 depicts tendency of t_{33}, φ and N vs. x_1 in case of NF with different values of kernel function for time delay $\omega = 0.05$. Near and far off the source, $Kernel - 3$ enhances the immensity of t_{33}.The behavior and variation of t_{33} for $Kernel - 1, Kernel - 2$ and $Kernel - 4$ is opposite oscillatory to $Kernel - 3$. The curve corresponds to t_{33} is fluctuating in nature for all values of kernel. Immensity of φ is higher due to $Kernel - 4$ and lower due to $Kernel - 1$ for the whole range of x_1. Near the source, $Kernel - 4$ enhances the value of N whereas minimum value is attained due to $Kernel - 2$. The style and fluctuations of φ and N are similar.

Figs. 1.4-1.6 shows movement of t_{33}, φ and N vs. x_1 in case of TS with different values of kernel function for time delay $\omega = 0.05$. Near the source, $Kernel - 1$ intensify the immensity of

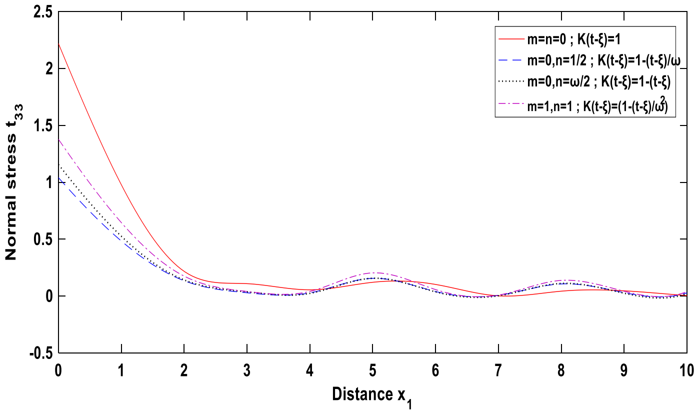

Fig. 1.4 Profile of t_{33} vs x_1 (TS with different values of kernel)

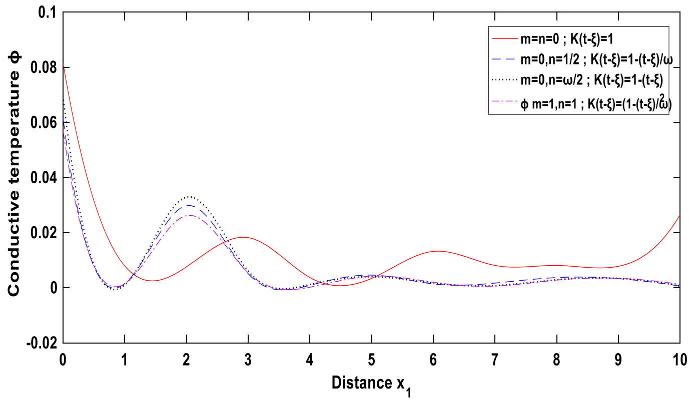

Fig. 1.5 Profile of ϕ vs x_1 (TS with different values of kernel)

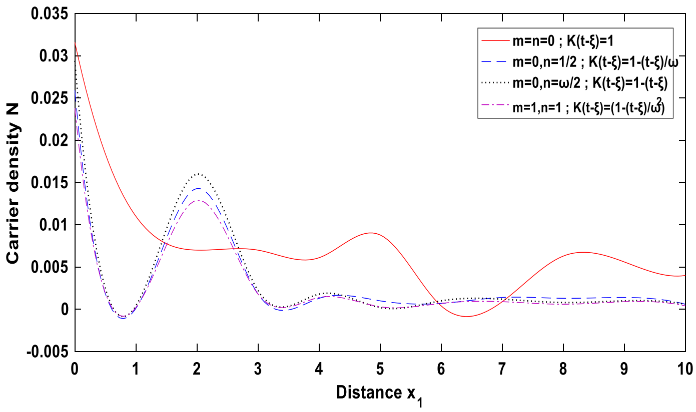

Fig. 1.6 Profile of N vs x_1 (TS with different values of kernel)

all components. All the physical quantities decrease monotonically in the initial range of distance x_1 and the values of quantities approaches zero for all values of kernel, when distance x_1 increases

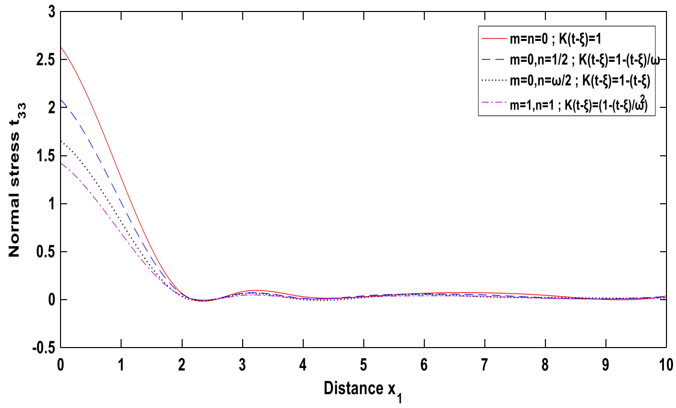

Fig. 1.7 Profile of t_{33} vs x_1 (CDS with different values of kernel)

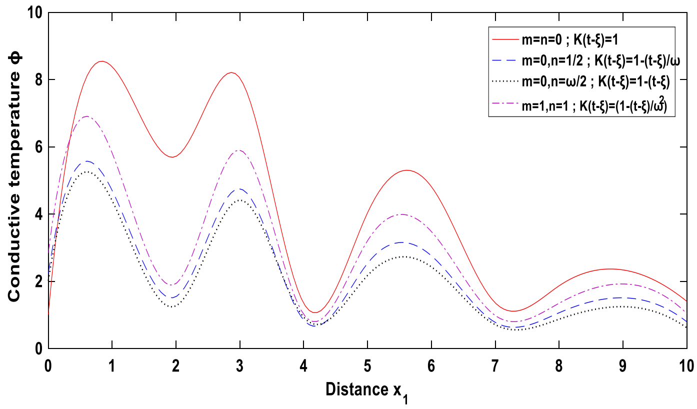

Fig. 1.8 Profile of ϕ vs x_1 (CDS with different values of kernel)

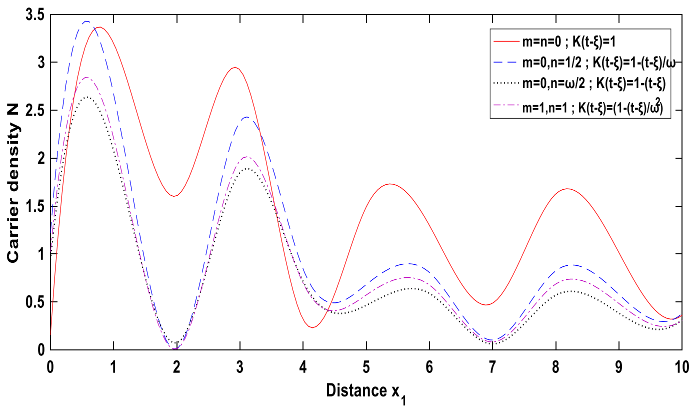

Fig. 1.9 Profile of N vs x_1 (CDS with different values of kernel)

further. Far off the source, the behavior of φ and N is in decreasing order due to $Kernel-2, Kernel-3$ and $Kernel-4$ and increasing order for $Kernel-1$.

Figs. 1.7-1.9 displays movement of t_{33}, φ and N vs. x_1 in case of CDS with different values of kernel function for time delay $\omega = 0.05$. t_{33} starts from its maxima and decreases with an increase in distance x_1 for all values of kernel. All curves correspond to t_{33} decreases to zero, which indicates lack of stress as distance increases. The immensity of φ and N starts from its minima and increases for large values of x_1

Case-II: Figs. 1.10-1.18 depict the variations of all field variables with distance x_1 on the plane $x_3 = 1$ for the different values of DPL.

Figs. 1.10-1.12 represent normal force (NF), Figs. 1.13-1.15 represents thermal source (TS), Figs. 1.16-1.18 represent carrier density source (CDS) for the fixed value of kernel function $K(t,\xi) = \left(1 - \frac{t-\xi}{\omega}\right)^2 \, if m = n = 1$. In all the Figs. solid line correspond to $\tau_T = 0.02, \tau_q = 0.05$ with MDD, dashed line corresponds to $\tau_T = 0.05, \tau_q = 0.08$ with MDD, dotted line corresponds to $\tau_T = 0.02, \tau_q = 0.05$ without MDD and dash-dot line corresponds to $\tau_T = 0.05, \tau_q = 0.08$ without MDD.

Figs. 1.10-1.12 depicts movement of t_{33}, φ and N vs. x_1 in case of NF with different values of DPL with and without MDD. Near and far off the source, absence of MDD raises the immensity of

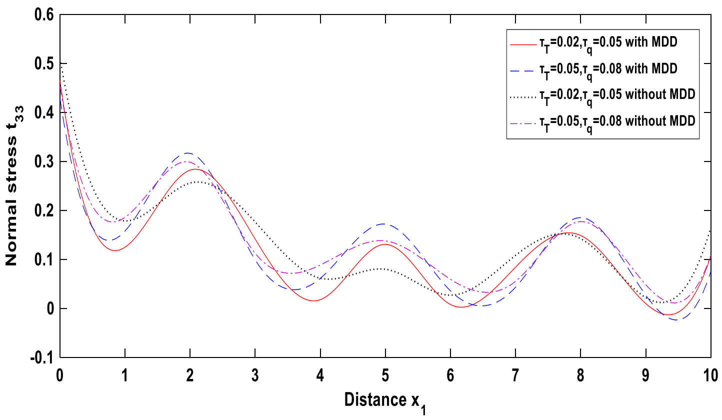

Fig. 1.10 Profile of t_{33} vs x_1 (NF with DPL)

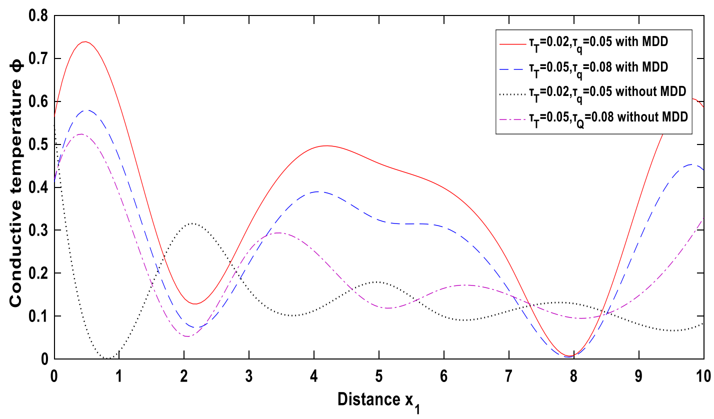

Fig. 1.11 Profile of ϕ vs x_1 (NF with DPL)

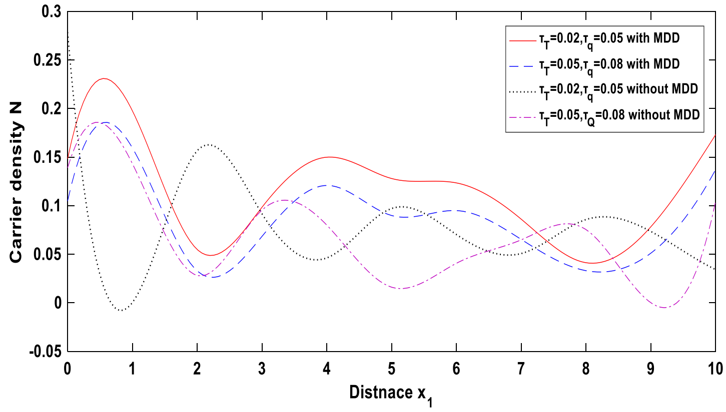

Fig. 1.12 Profile of N vs x_1 (NF with DPL)

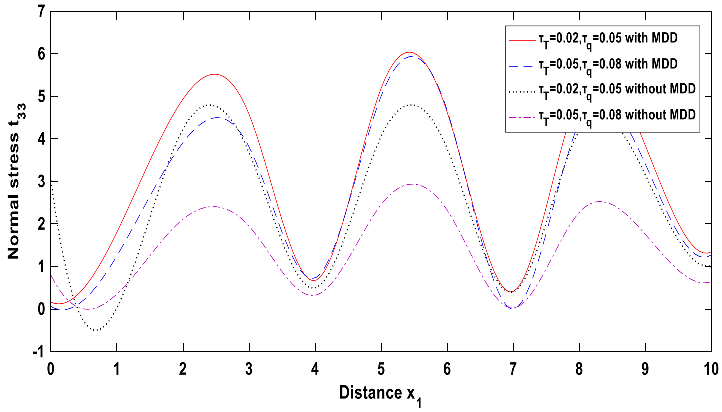

Fig. 1.13 Profile of t_{33} vs x_1 (TS with DPL)

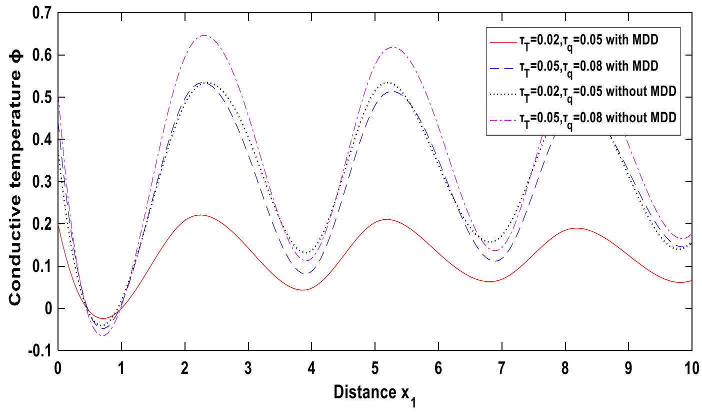

Fig. 1.14 Profile of ϕ vs x_1 (TS with DPL)

t_{33} when $\tau_T = 0.02, \tau_q = 0.05$ and presence of MDD minimizes the values of t_{33} with $\tau_T = 0.02, \tau_q = 0.05$. All the curves related to t_{33} for DPL model whether or not included MDD attain

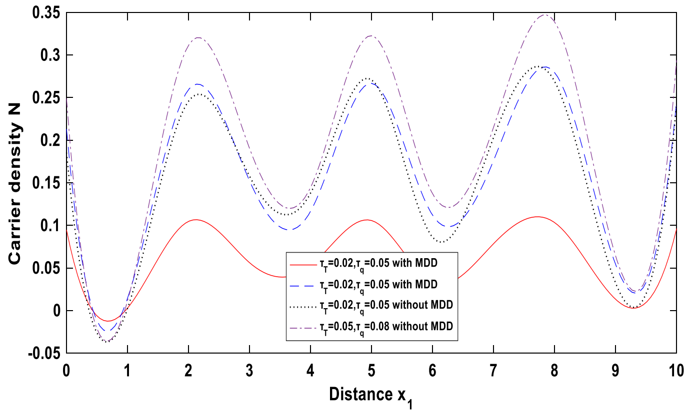

Fig. 1.15 Profile of N vs x_1 (TS with DPL)

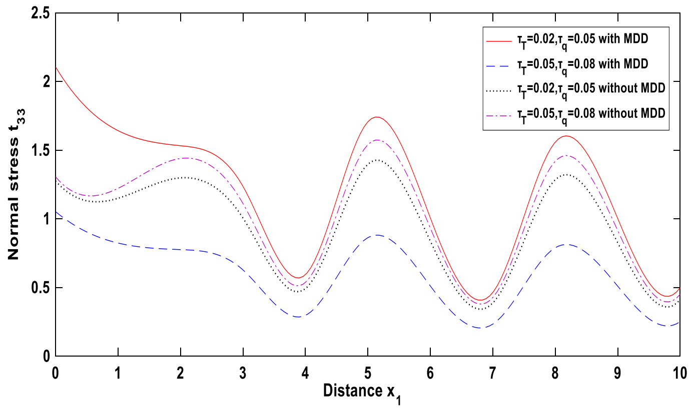

Fig. 1.16 Profile of t_{33} vs x_1 (CDSwith DPL)

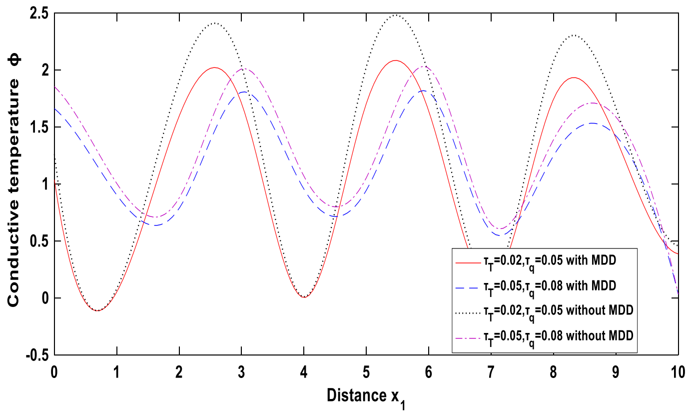

Fig. 1.17 Profile of ϕ vs x_1 (CDS with DPL)

inconsistent behavior for the whole range of x_1. The immensity of φ remains higher for $\tau_T = 0.02, \tau_q = 0.05$ in presence of MDD for the whole range of x_1. Near the source, DPL model $\tau_T =$

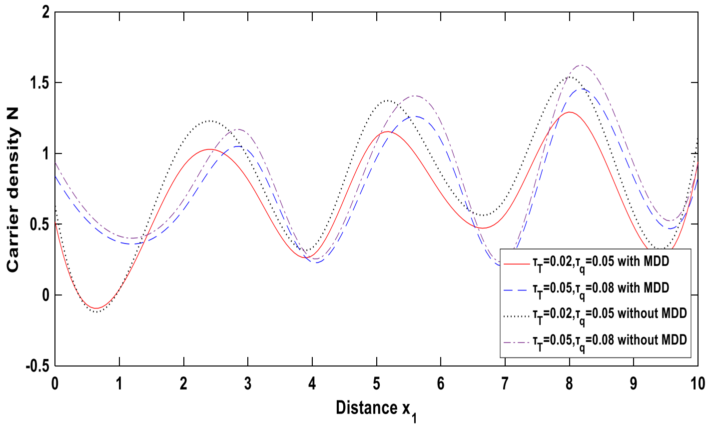

Fig. 1.18 Profile of N vs x_1 (CDS with DPL)

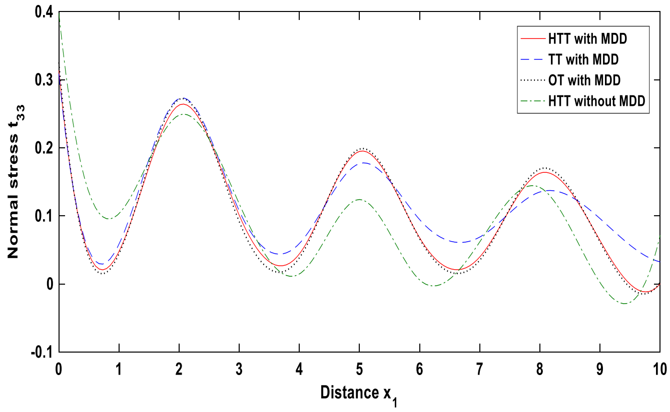

Fig. 1.19 Profile of t_{33} vs x_1 (NF with HTT)

$0.02, \tau_q = 0.05$ in absence of MDD maximize the values correspond to N. The behavior and variation of curve correspond to φ and N for $\tau_T = 0.02, \tau_q = 0.05$ without MDD is opposite oscillatory to all other curves of considered DPL model.

Figs. 1.13-1.15 shows movement of t_{33}, φ and N vs. x_1 in case of TS with distinct values of DPL with and without MDD. Initially, the magnitude of t_{33} enhances for $\tau_T = 0.02, \tau_q = 0.05$ in absence of MDD. On the other hand curve due to $\tau_T = 0.02, \tau_q = 0.05$ with MDD attain higher value of t_{33} for the entire range of x_1 as compare to other values of DPL model. The immensity of φ and N attain minima for DPL model for $\tau_T = 0.02, \tau_q = 0.05$ with MDD for the entire range of x_1 and similarly DPL model for $\tau_T = 0.05, \tau_q = 0.08$ without MDD intensify the values of φ and N.

Figs. 1.16-1.18 displays tendency of t_{33}, φ and N vs. x_1 in case of CDS with different values of DPL with and without MDD. The curves correspond to t_{33}, φ and N are in decreasing trend near the source and attain increasing trend far off the source. All curves with and without MDD based on DPL model, correspond to t_{33}, φ and N attain fluctuating behavior for the whole range of x_1.

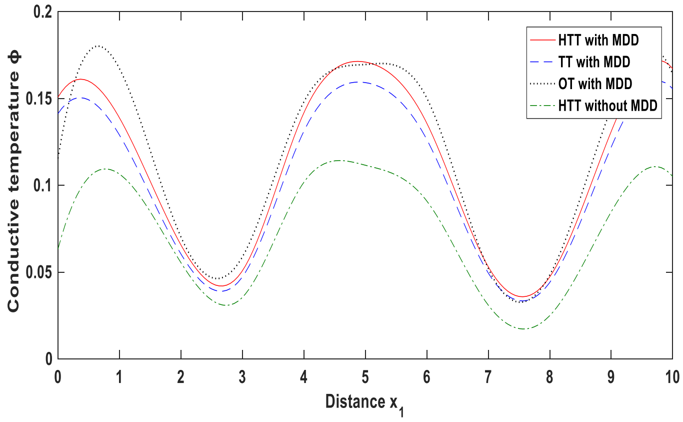

Fig. 1.20 Profile of ϕ vs x_1 (NF with HTT)

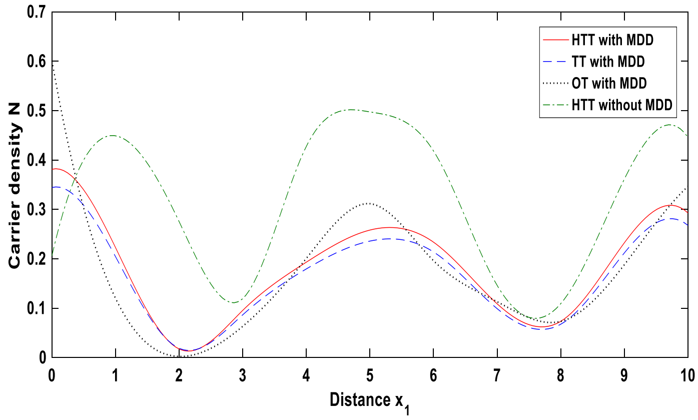

Fig. 1.21 Profile of N vs x_1 (NF with HTT)

Case-III: Figs. 1.19-1.27 depict the variations of all field variables with distance x_1 on the plane $x_3 = 1$ for the different values of HTT, TT and OT.

Figs. 1.19-1.21 represent normal force (NF), Figs. 1.22-1.24 represents thermal source (TS), Figs. 1.25-1.27 represent carrier density source (CDS) for the fixed value of kernel function $K(t,\xi) = \left(1 - \frac{t-\xi}{\omega}\right)^2$ $if m = n = 1$. In all the figures. solid line correspond HTT with MDD, dashed line corresponds to TT (two temperature) with MDD, dotted line corresponds to OT (one temperature) with MDD and dash-dot line corresponds to HTT without MDD.

Figs. 1.19-1.21 depicts movement of t_{33}, φ and N vs. x_1 in case of NF with and without MDD based on HHT, TT and OT. Near and far off the source, HTT in absence of MDD raises the immensity of t_{33}. The curves correspond to t_{33} for HTT and OT (with MDD) varies in same manner with minor difference in their immensity. Initially, the immensity of φ and N are intensify due to HTT (with MDD) and OT (with MDD) respectively. HTT (in absence of MDD) minimize the immensity of φ for the whole range of x_1 and maximize the value of N for $x_1 \geq 1$.

Figs. 1.22-1.24 demonstrates movement of t_{33}, φ and N vs. x_1 in case of TS with and without MDD based on HHT, TT and OT. Near the source, MDD based on TT maximize the immensity of

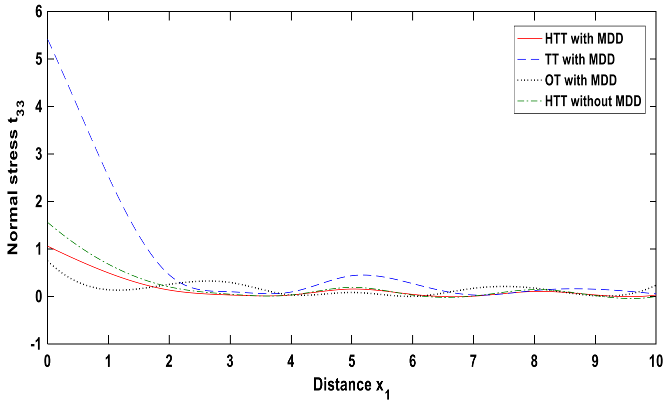

Fig. 1.22 Profile of t_{33} vs x_1 (TS with HTT)

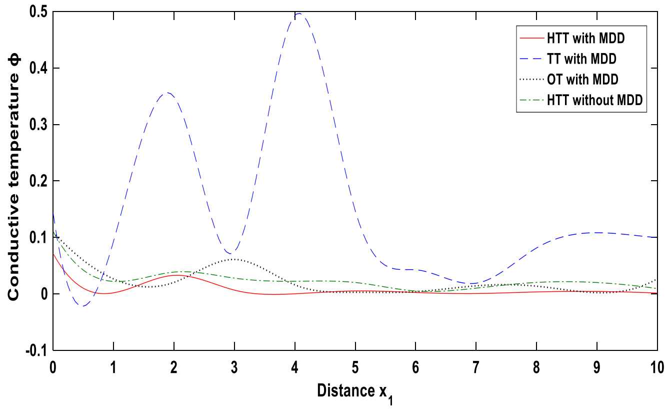

Fig. 1.23 Profile of ϕ vs x_1 (TS with HTT)

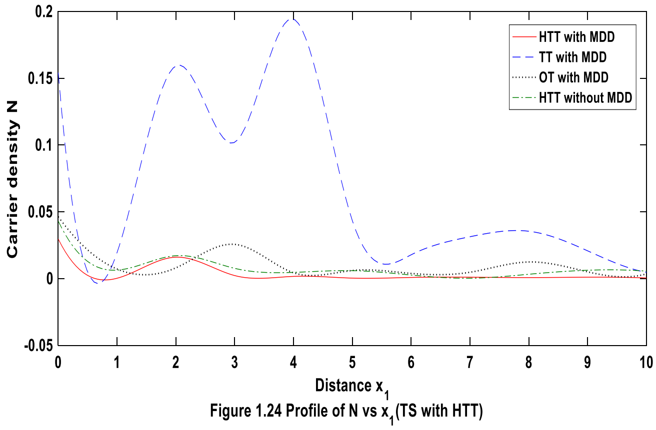

Fig. 1.24 Profile of N vs x_1 (TS with HTT)

t_{33} and monotonically decreases in the range $x_1 \geq 2$. The form and style of curves correspond to t_{33} for OT (with MDD) is opposite oscillatory with HTT (with and without MDD). The immensity

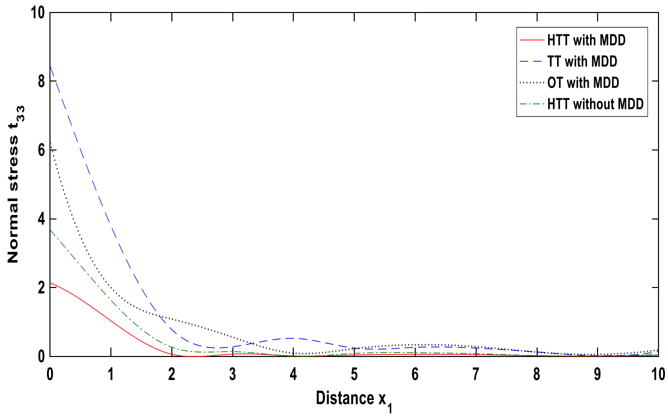

Fig. 1.25 Profile of t_{33} vs x_1 (CDS with HTT)

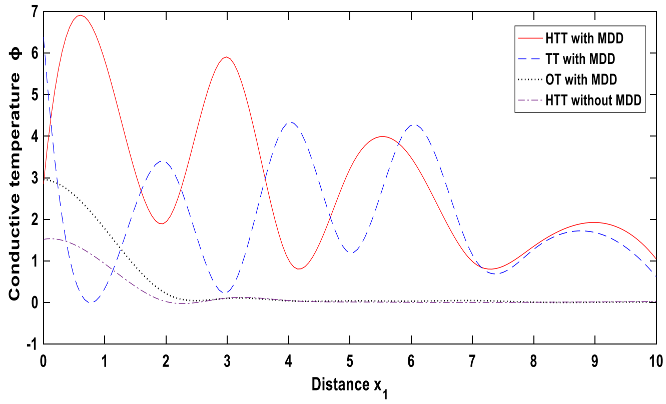

Fig. 1.26 Profile of ϕ vs x_1 (CDS with HTT)

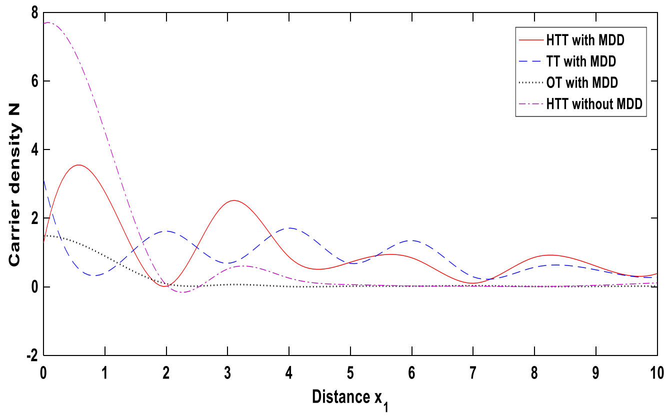

Fig. 1.27 Profile of N vs x_1 (CDS with HTT)

of φ and N is higher due to TT (with MDD) in the range $x_1 \geq 1$. The curves correspond to φ and N due to HTT (with and without MDD) and OT (with MDD) are less oscillatory as

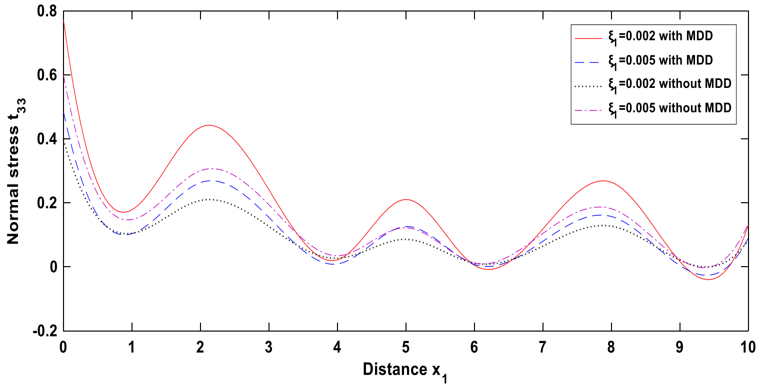

Fig. 1.28 Profile of t_{33} vs x_1 (NF with NL)

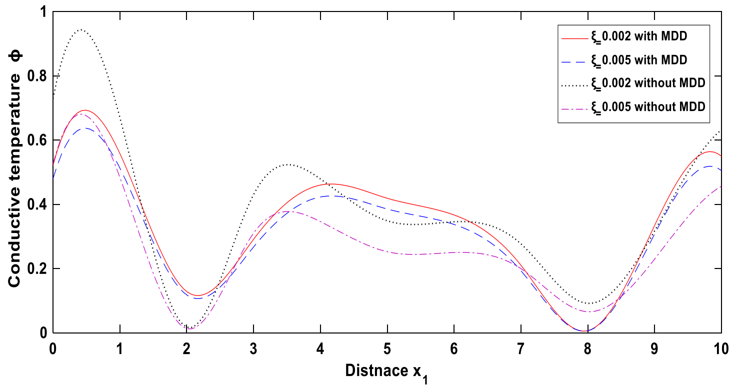

Fig. 1.29 Profile of ϕ vs x_1 (NF with NL)

compare to TT (with MDD).

Figs. 1.25-1.27 shows movement of t_{33}, φ and N vs. x_1 in case of CDS with and without MDD based on HHT, TT and OT. The magnitude of t_{33} attain decreasing trend for all the considered theories for the intermediate values of x_1. The values of t_{33} for HTT (with and without MDD), TT (with MDD) and OT (with MDD) oscillate close to zero with increase in distance. The curves correspond to φ and N behave opposite oscillatory for HTT (with MDD) and TT (with MDD), whereas curves for OT (with MDD) and HTT (without MDD) behave in similar way.

Case-IV: Figs. 1.28-1.36 depict the variations of all field variables with distance x_1 on the plane $x_3 = 1$ for the different values of non-local parameter.

Figs. 1.28-1.30 represent normal force (NF), Figs. 1.31-1.33 represents thermal source (TS), Figs. 1.34-1.36 represent carrier density source (CDS) for the fixed value of kernel function $K(t,\xi) = \left(1 - \frac{t-\xi}{\omega}\right)^2 if m = n = 1$. In all the figures solid line corresponds to $\xi_1 = 0.002$ with MDD, dashed line corresponds to $\xi_1 = 0.002$ with MDD, dotted line correspond to $\xi_1 = 0.005$ without MDD and dash-dot line corresponds to $\xi_1 = 0.005$ without MDD.

Figs. 1.28-1.30 depicts movement of t_{33}, φ and N vs. x_1 in case of NF with and without MDD based on NL parameter. Near the source, NL parameter $\xi_1 = 0.002$ in presence of MDD intensify the magnitude of t_{33}, whereas $\xi_1 = 0.002$ in absence of MDD attain minimum value. All the

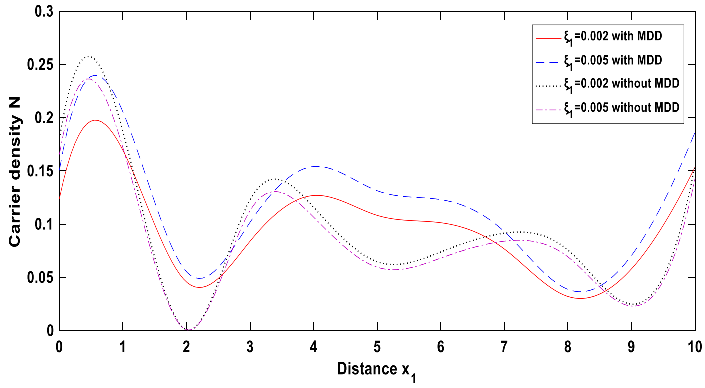

Fig. 1.30 Profile of N vs x_1 (TS with NL)

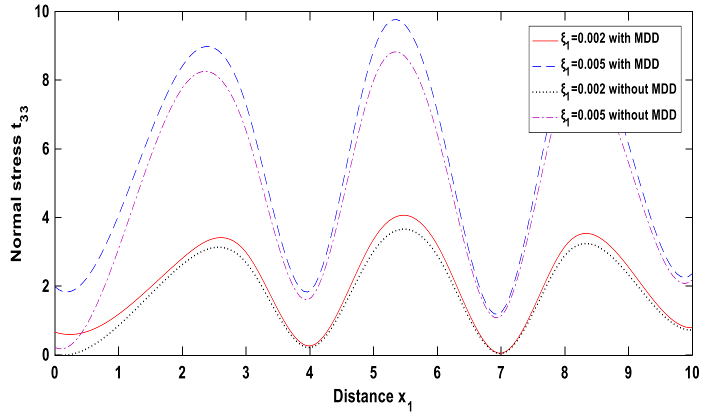

Fig. 1.31 Profile of t_{33} vs x_1 (TS with NL)

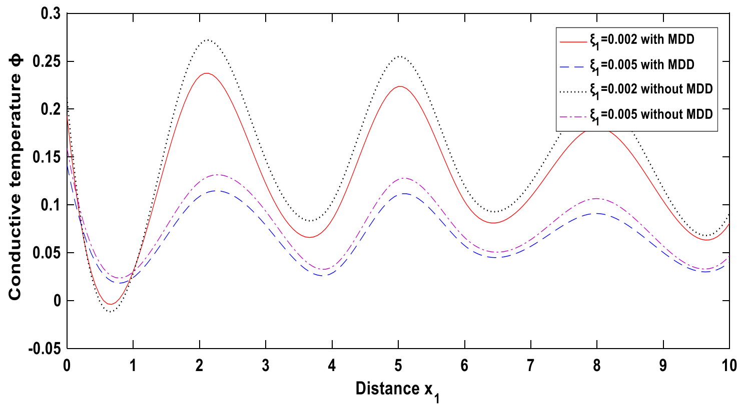

Fig. 1.32 Profile of ϕ vs x_1 (TS with NL)

curves correspond to t_{33} be fluctuating in nature for the whole range of x_1. In the initial range of x_1,φ and N attain higher value due to NL parameter $\xi_1 = 0.002$ with MDD. The style and fluctuation of curves correspond to φ and N be opposite oscillatory for $\xi_1 = 0.002$ & $\xi_1 = 0.005$

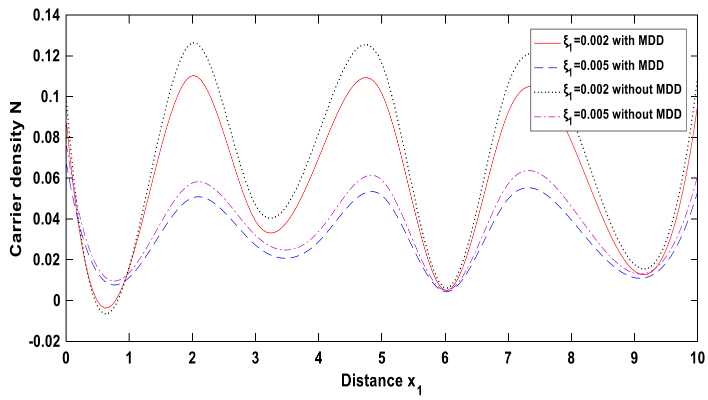

Fig. 1.33 Profile of N vs x_1 (TS with NL)

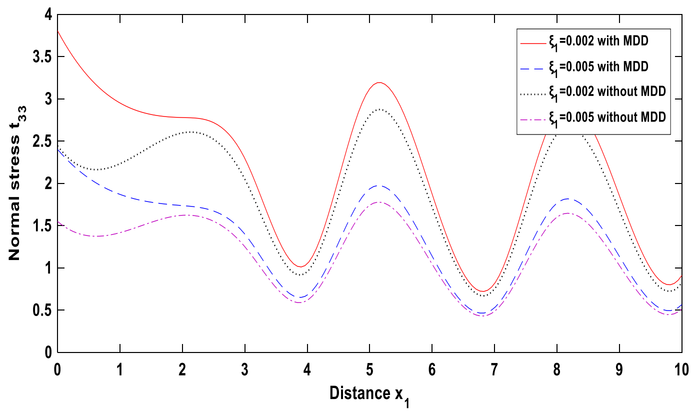

Fig. 1.34 Profile of t_{33} vs x_1 (CDS with NL)

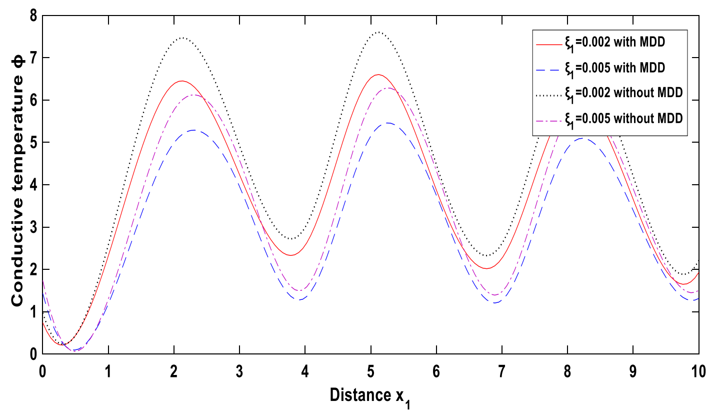

Fig. 1.35 Profile of ϕ vs x_1 (CDS with NL)

(with MDD) and $\xi_1 = 0.002$ & $\xi_1 = 0.005$ (without MDD) for the intermediate values of x_1.

Figs. 1.31-1.33 demonstrate movement of t_{33}, φ and N vs. x_1 in case of TS with and without MDD based on NL parameter. The immensity of t_{33} attain maxima due to $\xi_1 = 0.005$ (with

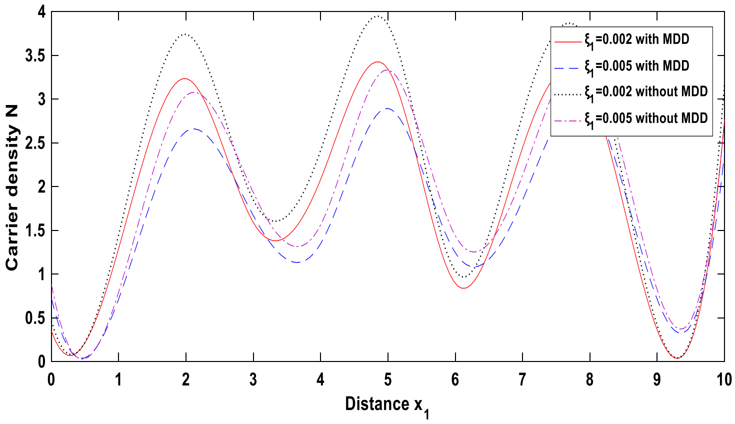

Fig. 1.36 Profile of N vs x_1 (CDS with NL)

MDD) and minima due to $\xi_1 = 0.002$ (without MDD) for the whole range of x_1. The behavior and variation of t_{33} is similar for $\xi_1 = 0.002$ & $\xi_1 = 0.005$ (with MDD) and $\xi_1 = 0.002$ & $\xi_1 = 0.005$ (without MDD) with distinct immensities. NL parameter $\xi_1 = 0.002$ (without MDD) raises the immensity of φ and N. Increase in value of NL parameter (with or without MDD), decreases the value of φ and N.

Figs. 1.34-1.36 shows movement of t_{33}, φ and N vs. x_1 in case of CDS with and without MDD based on NL parameter. The immensity of t_{33} attain maxima due to $\xi_1 = 0.002$ (with MDD) and minima due to $\xi_1 = 0.005$ (without MDD) for the whole range of x_1. Increase in value of NL parameter (with or without MDD), decreases the value of t_{33}. NL parameter $\xi_1 = 0.002$ (without MDD) raises the immensity of φ and N for the intermediate values of x_1. The immensity of φ and N is higher for lower value of NL parameter in absence of MDD.

9. Conclusions

In this paper a new mathematical model on PMDD based on NL, DPL and HTT has been established to examine the two-dimensional problem in half-space. Integral transform (Laplace and Fourier) compact the system of equations into ordinary differential equation. Specific types of sources are taken to establish the applicability of the problem. The transformed expressions are converted into the physical domain by using numerical technique and presented in the form of figures. After the numerical results the following conclusions are made:

• In case of NF, the form and design of t_{33} is opposite oscillatory for $Kernel - 3$ to $Kernel - 1,2,4$. The curves correspond to φ and N fluctuate in similar manner with finite difference in their immensity. Monotonically decreasing behavior is noticed in initial range of x_1 for all values of kernel function correspond to t_{33}, φ and N for TS. In case of CDS, t_{33} starts with its maximum value and decreases monotonically in certain range of x_1. φ and N get maxima due to $Kernel - 1$ as compare to other values of kernel function.

• The curve correspond to t_{33} attains maximum immensity near and far off the source due to DPL in absence of MDD, whereas curves for $\varphi and N$is opposite oscillatory for DPL in absence of MDD for NF. In case of TS, t_{33}, φ and N fluctuate in similar manner for all assumed values of DPL model in presence and absence of MDD. Immensity of t_{33} raises due to DPL with MDD, whereas immensity of φ and N enhances due to DPL without MDD for CDS.

• The curves correspond to t_{33} starts with its maximum value and decreases monotonically in initial range of x_1 and then oscillate for whole range of x_1 due to HTT (with and without MDD) for NF. Due to HTT without MDD, φ gets minimum value for entire range of x_1 and N attain maximum value for $x_1 \geq 1$ in case of NF. Near the source, t_{33} attain maxima due to TT (with MDD) and minima when OT (with MDD) for TS. TT (with MDD) enhances the magnitude of φ and N for intermediate values of distance, whereas other curves travel with less variation in case of TS. In case of CDS, t_{33} behaves in same manner as TS with difference in magnitude and the behavior of φ and N are opposite oscillatory for HTT and TT (with MDD), whereas curves for OT (with MDD) and HTT (without MDD) tends to zero as distance increases.

• All the curves correspond to t_{33} be fluctuating in nature for the whole range of x_1. The form and design of curves correspond to φ and N be opposite oscillatory due to NL parameter (with and without MDD) for NF. In case of TS, the immensity of t_{33} attain maxima due to higher value of NL parameter in presence of MDD and gets minima due to lowest value of NL parameter in absence of MDD for the whole range of x_1. φ and N gets maxima for small value of NL parameter for TS. Increase in value of NL parameter (with or without MDD), decreases the value of t_{33} and the values of φ and N is maximum in absence of MDD, whereas presence of MDD enhances the magnitude for CDS.

It is concluded that normal stress, conductive temperature and carrier density distribution show sporadic format for normal force, thermal source and carrier density source based on different values of kernel function, NL, DPL and HTT (with and without MDD) with respect to distance x_1. It is observed that NL, DPL and HTT have significant effect on resulting quantities. The photothermal process considered in this problem has many applications in physical engineering, physical chemistry and medical physics. Mathematical model persist in this article is useful modern tool for scientific investigation of different photothermoelastic problems. It is also concluded that the system of equation in this work will be prove to be valuable for understanding the combined impact of photothermoelasticity under NL, DPL and HTT with MDD. Which determine the characteristics of various bodies in important engineering problems. MDD can be used to reclassify the semiconductor materials in terms of photo elastic thermal conductivity. The Work presented in this model can be applied to thermoelastic material with nanostructure and plasmonic structure.

References

Abo Dahab, S.M., Lotfy, Kh. and Gohaly, A. (2015), "Rotation and magnetic field effect on surface waves propagation in an elastic layer lying over a generalized thermoelastic diffusive half-space with imperfect boundary", *Math. Prob. Eng.*, **2015**(1), 671783. https://doi.org/10.1155/2015/671783.

Abo-Dahab, S. and Lotfy, Kh. (2015), "Generalized magneto-thermoelasticity with fractional derivative heat transfer for a rotation of a fibre-reinforced thermoelastic", *J. Comput. Theor. Nanosci.*, **12**(8), 1869-1881. https://doi.org/10.1166/jctn.2015.3972.

Abouelregal, A., Marin, M. and Öchsner, A. (2023), "The influence of a non-local Moore-Gibson-Thompson heat transfer model on an underlying thermoelastic material under the model of memory-dependent derivatives", *Contin. Mech. Thermodyn.*, **35**(2), 545-562. https://doi.org/10.1007/s00161-023-01195-y.

Abouelregal, A.E. and Dargail, H.E. (2021), “Memory and dynamic response of a thermoelastic functionally graded nanobeams due to a periodic heat flux”, *Mech. Bas. Des. Struct. Mach.*, **51**(4), 2154-2176. https://doi.org/10.1080/15397734.2021.1890616.

Abouelregal, A.E., Atta, D. and Sedighi, H.M. (2023), “Vibrational behavior of thermoelastic rotating nanobeams with variable thermal properties based on memory-dependent derivative of heat conduction model”, *Arch. Appl. Mech*., **93**, 197-220. https://doi.org/10.1007/s00419-022-02110-8.

Abouelregal, A.E., Civalek, Ö. and Akgöz, B. (2025), “A size-dependent non-fourier heat conduction model for magneto-thermoelastic vibration response of nanosystems”, *J. Appl. Comput. Mech.*, **11**(2), 344-357. https://doi.org/10.22055/jacm.2024.46746.4584.

Abouelregal, A.E., Marin, M., Askar, S.S. and Foul, A. (2024), “Transient thermoelastic response in a semi-infinite medium subjected to a moving heat source: An implementation of the Moore-Gibson-Thompson model with higher-order memory-dependent derivatives”, *Mech. Time-depend. Mater.*, **28**(3), 1555-1581. https://doi.org/10.1007/s11043-024-09672-w.

Almond, D.P. and Patel, P.M. (1996), *Photothermal Science and Techniques*, Chapman and Hall, London.

Biot, M.A. (1956), “Thermoelasticity and irreversible thermodynamics”, *J. Appl. Phys.*, **27**(3), 240-253. https://doi.org/10.1063/1.1722351.

Caputo, M. (1967), “Linear models of dissipation whose Q is almost frequency independent—II”, *Geophys. J. Int.*, **13**(5), 529-539. https://doi.org/10.1111/j.1365-246X.1967.tb02303.x.

Diethelm, K. (2010), *Analysis of Fractional Differential Equation: An Application- Oriented Exposition Using Differential Operators of Caputo Type*, Springer, Berlin, Heideberg.

Ezzat, M.A., El-Karamany, A.S. and El-Bary, A.A. (2014), “Generalized thermoviscoelasticity with memory dependent derivatives”, *Int. J. Mech. Sci.*, **89**, 470-475. https://doi.org/10.1016/j.ijmecsci.2014.10.006.

Ezzat, M.A., El-Karamany, A.S. and El-Bary, A.A. (2015), “A novel magneto thermoelasticity theory with memory dependent derivative”, *J. Electromagnet. Wave. Appl.*, **29**(8), 1018-1031. https://doi.org/10.1080/09205071.2015.1027795.

Ezzat, M.A., El-Karamany, A.S. and El-Bary, A.A. (2016), “Generalized thermoelasticity with memory-dependent derivatives involving two-temperatures”, *Mech. Adv. Mater. Struct.*, **23**, 545-553. https://doi.org/10.1080/15376494.2015.1007189.

Green, A.E. and Naghdi, P.M. (1991), “A re-examination of the basic postulates of thermomechanics”, *Proc. Roy. Soc. London. Ser. A: Math. Phys. Sci.*, **432**(1885), 171-194. https://doi.org/10.1098/rspa.1991.0012.

Green, A.E. and Naghdi, P.M. (1992), “On undamped heat waves in an elastic solid”, *J. Therm. Stress*., **15**, 253-264. https://doi.org/10.1080/01495739208946136.

Green, A.E. and Naghdi, P.M. (1993), “Thermoelasticity without energy dissipation”, *J. Elast*., **31**(3), 189-208. https://doi.org/10.1007/BF00044969.

Hendy, M.H., El-Attar, S.I. and Ezzat, M.A. (2020), “On thermoelectric materials with memory- dependent derivative and subjected to a moving heat source”, *Microsyst. Technol*., **26**, 595-608. https://doi.org/10.1007/s00542-019-04519-8.

Honig, G. and Hirdes, U. (1984), “A method for the numerical inversion of Laplace transforms”, *J. Comput. Appl. Math.*, **10**(1), 113-132. https://doi.org/10.1016/0377-0427(84)90075-X.

Jackson, W. and Amer, N.M. (1980), “Piezoelectric photoacoustic detection: Theory and experiment”, *J. Appl. Phys*., **51**(6), 3343-3353. https://doi.org/10.1063/1.328045.

Jahangir, A., Tanvir, F. and Zenkour, A.M. (2020), “Reflection of photothermoelastic waves in a semiconductor material with different relaxations”, *Ind. J. Phys.*, **95**, 51-59. https://doi.org/10.1007/s12648-020-01690-x.

Kumar, R., Sharma, N. and Chopra, S. (2022), “Modelling of thermomechanical response in anisotropic photothermoelastic plate”, *Int. J. Mech. Eng.*, **7**(6), 577-594.

Kumar, R., Sharma, N. and Chopra, S. (2022), “Photothermoelastic interations under Moore- Gibson-Thompson thermoelasticity”, *Couple. Syst. Mech.*, **11**(5), 459-483. https://doi.org/10.12989/csm.2022.11.5.459.

Lord, H.W. and Shulman, Y. (1967), “A generalized dynamical theory of thermoelasticity”, *J. Mech. Phys.*

Solid., **15**(5), 299-309. https://doi.org/10.1016/0022-5096(67)90024-5.

Lotfy, K. and Tantawi, R.S. (2020), “Photo-thermal-elastic interaction in a functionally graded material (FGM) and magnetic field”, *Silicon*, **12**, 295-303. https://doi.org/10.1007/s12633-019-00125-5.

Lotfy, K., El-Bary, A.A. and Tantawi, R.S. (2019), “Effects of variable thermal conductivity of a small semiconductor cavity through the fractional order heat-magneto-photothermal theory”, *Eur. Phys. J. Plus*, **134**, 280. https://doi.org/10.1140/epjp/i2019-12631-1.

Lotfy, Kh. (2012), “Mode-I crack in a two-dimensional fibre-reinforced generalized thermoelastic problem”, *Chin. Phys. B.*, **21**, 014209. https://doi.org/10.1088/1674-1056/21/1/014209.

Lotfy, Kh., Elidy, E. and Tantawi, R. (2021), “Piezo-photo-thermoelasticity transport process for hyperbolic two-temperature theory of semiconductor material”, *Int. J. Mod. Phys. C*, **32**(07), 2150088. https://doi.org/10.1142/S0129183121500881.

Lotfy, Kh., Kumar, R., Hassan, W. and Gabr, M. (2018), “Thermomagnetic effect with microtemperature in a semiconducting photothermal excitation medium”, *Appl. Math. Mech.*, **39**, 783-796. https://doi.org/10.1007/s10483-018-2339-9.

Mahdy, A., Gepreel, Kh., Lotfy, Kh. and El-Bary, A. (2021), “A numerical method for solving the Rubella ailment disease model”, *Int. J. Mod. Phys. C*, **32**(07), 2150097. https://doi.org/10.1142/S0129183121500972.

Mahdy, A., Mohamed, M.S., Lotfy, Kh., Alhazmi, M., El-Bary, A.A. and Raddadi, M.H. (2021), “Numerical solution and dynamical behaviors for solving fractional nonlinear Rubella ailment disease model”, *Result. Phys.*, **24**(21), 2211-3797. https://doi.org/10.1016/j.rinp.2021.104091.

Mandelis, A. (1987), *Photoacoustic and Thermal wave Phenomena in Semiconductors*, Elsevier Science, North- Holland, New York.

Mandelis, A. and Michaelian, K.H. (1997), “Photoacoustic and photothermal science and engineering” *Opt. Eng.*, **36**(2), 301-302.

McDonald, F.A. and Wetsel, G.C. (1978), “Generalized theory of the photoacoustic effect”, *J. Appl. Phys.*, **49**(4), 2313-2322. https://doi.org/10.1063/1.325116.

Nikolic, P.M. and Todorovic, D.M. (1989), “Photoacoustic and electroacoustic properties of semiconductors”, *Prog. Quantum. Electron.*, **13**, 107-189.

Sharma, K. (2010), “Boundary value problems in generalised thermodiffusive elastic medium”, *J. Solid Mech.*, **2**(4), 348-362.

Sharma, N. and Kumar, R. (2021), “Photo-thermoelastic investigation of semiconductor material due to distributed loads”, *J. Solid Mech.*, **13**(2), 202-212. https://doi.org/10.22034/jsm.2020.1907462.1639.

Sharma, N. and Kumar, R. (2022), “Photothermoelastic deformation in dual phase lag model due to concentrated inclined load”, *Ital. J. Pure Appl. Math.*, **48**, 1147-1160.

Sharma, S. and Khator, S. (2021), “Power generation planning with reserve dispatch and weather uncertainties including penetration of renewable sources”, *Int. J. Smart Grid Clean Energy*, **10**(4), 292-303. https://doi.org/10:12720/sgce10.4.

Sharma, S. and Khator, S. (2022), “Micro- Grid planning with aggregator’s role in the renewable inclusive pro sumer market”, *J. Power Energy Eng.*, **10**(4), 47-62. https://doi.org/10.4236/jpee.2022-10404.

Sharma, S. and Sharma, K. (2014), “Influence of heat sources and relaxation time on temperature distribution in tissues”, *Int. J. Appl. Mech. Eng.*, **19**(2), 427-433. https://doi.org/10.2478/ijame-2014-0029.

Sharma, S., Sharma, K. and Bhargava, R.R. (2013), “Effect of viscosity on wave propagation in anisotropic thermoelastic with Green-Naghdi theory type-II and type- III”, *Mater. Phys. Mech.*, **16**(2), 144-158.

Stearns, R. and Kino, G. (1985), “Effect of electronic strain on photoacoustic generation in silicon”, *Appl. Phys. Lett.*, **47**(10), 1048-1050. https://doi.org/10.1063/1.96374.

Todorović, D.M. (2003), “Photothermal and electronic elastic effects in microelectromechanical structures”, *Rev. Scientif. Instrum.*, **74**(1), 578-581. https://doi.org/10.1063/1.1520324.

Todorović, D.M. (2005), “Plasmaelastic and thermoelastic waves in semiconductors”, *J. Physique IV*, **125**, 551-555. https://doi.org/10.1051/jp4:2005125127.

Tzou, D.Y. (1995), “A unified approach for heat conduction from macro-to-micro- scales”, *J. Heat Transf.*, **117**(1), 8-16. https://doi.org/10.1115/1.2822329.

Wang, J. and Li, H. (2011), "Surpassing the fractional derivative: Concept of the memory-dependent derivative", *Comput. Math. Appl.*, **62**(3), 1562-1567. https://doi.org/10.1016/j.camwa.2011.04.028.

Yu, Y.J., Hu, W. and Tian, X.G. (2014), "A novel generalized thermoelasticity model based on memory-dependent derivative", *Int. J. Eng. Sci.*, **81**, 123-134. https://doi.org/10.1016/j.ijengsci.2014.04.014.

Zakaria, K., Sirwah, M.A. and Abouelregal, A.E. (2021), "Photo-thermoelastic model with time-fractional of higher order and phase lags for a semiconductor rotating materials", *Silicon*, **13**, 573-585. https://doi.org/10.1007/s12633-020-00451-z.

Zenkour, A.M. (2020), "Exact coupled solution for photothermal semiconducting beams using a refined multi- phase-lag theory", *Opt. Laser Technol.*, **128**, 106233. https://doi.org/10.1016/j.optlastec.2020.106233.